AMERICAN SOCIETY FOR MICROBIOLOGY | Journal of Virology®

STRUCTURE AND ASSEMBLY

The Autographa californica Multiple Nucleopolyhedrovirus *ac51* Gene Is Required for Efficient Nuclear Egress of Nucleocapsids and Is Essential for *In Vivo* Virulence

Jianxiang Qiu,[a] Zhimin Tang,[a] Yi Cai,[a] Wenbi Wu,[a] Meijin Yuan,[a] Kai Yang[a]

[a]State Key Laboratory of Biocontrol, Sun Yat-sen University, Guangzhou, China

ABSTRACT Alphabaculoviruses are lepidopteran-specific nucleopolyhedroviruses that replicate within the nucleus; however, the anterograde transport of the nucleocapsids of these viruses, which is an obligatory step for progeny virion production, is not well understood. In the present study, a unique *Alphabaculovirus* gene with unknown function, namely, the Autographa californica multiple nucleopolyhedrovirus (AcMNPV) *ac51* gene, was found to be required for efficient nuclear egress of AcMNPV nucleocapsids. Our results indicate that *ac51* is a late gene, and Ac51 protein was detectable from 24 to 72 h postinfection using an antibody raised against Ac51. Ac51 is distributed in both the cytoplasm and nuclei of infected cells. Upon *ac51* deletion, budded virion (BV) production by 96 h posttransfection was reduced by approximately 1,000-fold compared with that of wild-type AcMNPV. Neither viral DNA synthesis nor viral gene expression was affected. Ac51 was demonstrated to be a nucleocapsid protein of BVs, and *ac51* deletion did not interrupt nucleocapsid assembly and occlusion-derived virion (ODV) formation. However, BV production in the supernatants of transfected cells during a viral life cycle was substantially decreased when *ac51* was deleted. Further analysis showed that, compared with wild-type AcMNPV, *ac51* deletion decreased nucleocapsid egress, while the numbers of nucleocapsids in the nuclei were comparable. Deletion of *ac51* also eliminated the virulence of AcMNPV *in vivo*. Taken together, our results support the conclusion that *ac51* plays an important role in the nuclear egress of nucleocapsids during BV formation and is essential for the *in vivo* virulence of AcMNPV.

KEYWORDS Ac51, baculovirus, nuclear transport, nucleocapsid

Little is known about the mechanism underlying the nuclear egress of baculovirus nucleocapsids. In particular, the mechanism by which nucleocapsids of alphabaculoviruses efficiently egress from the nucleus to produce high levels of budded virions (BVs) in cultured cells is not known. Some genes that are conserved in all baculoviruses have been identified as essential for not only the nuclear egress of nucleocapsids, but also occlusion-derived virion (ODV) formation. In this study, we show that *ac51*, a unique *Alphabaculovirus* gene, encodes a nucleocapsid protein of BVs and is required for high levels of BV production. Deletion of the gene impaired efficient nuclear egress of nucleocapsids, but not nucleocapsid assembly or ODV formation, which is similar to the phenotype observed for *ac141* or *ac66* deletion. This result indicated that Ac51 is the third nucleocapsid protein that promotes the nuclear egress of nucleocapsids by a common pathway with Ac141 and Ac66.

Most DNA viruses, such as herpesviruses, ebolaviruses, and baculoviruses, replicate and assemble their nucleocapsids in the nuclei of host cells (1–3). The transport of nucleocapsids from the assembly sites in the nucleus to the budding sites at the plasma membrane within infected cells is an obligatory step of viral maturation. This process

Citation Qiu J, Tang Z, Cai Y, Wu W, Yuan M, Yang K. 2019. The Autographa californica multiple nucleopolyhedrovirus *ac51* gene is required for efficient nuclear egress of nucleocapsids and is essential for *in vivo* virulence. J Virol 93:e01923-18. https://doi.org/10.1128/JVI.01923-18.

Editor Rozanne M. Sandri-Goldin, University of California, Irvine

Address correspondence to Kai Yang, yangkai@mail.sysu.edu.cn.

Received 30 October 2018
Accepted 30 October 2018
Accepted manuscript posted online 14 November 2018
Published 17 January 2019

is called viral anterograde transport and is important for viral pathogenicity; the pathway is also a good target for disrupting viral infection.

Baculoviruses, which are a diverse group of enveloped viruses with circular double-stranded DNA genomes ranging from 80 to 180 kb in size, are specifically pathogenic toward insects, mainly those belonging to the orders Lepidoptera, Hymenoptera, and Diptera (4, 5). Alphabaculoviruses (lepidopteran-specific nucleopolyhedroviruses) and betabaculoviruses (lepidopteran-specific granuloviruses) produce two types of morphologically distinct but genetically identical progeny virions in a single viral life cycle: BVs and ODVs. After nucleocapsids enter the host cells and viral DNA is released in the nuclei, immediate-early gene expression, delayed early gene expression, viral DNA replication, and late gene expression occur sequentially (6, 7). Meanwhile, the formation of a virogenic stroma (VS) is induced in the center of the nucleus. Upon the production of late viral gene products, nucleocapsids assemble in the VS. For BV formation, synthesized nucleocapsids are transported out of the VS to the nuclear periphery (the so-called ring zone) and then penetrate the nuclear membrane (NM), transit through the cytoplasm (Cyt), and finally bud from the plasma membrane to form BVs. Subsequently, during infection, nucleocapsids are retained in the nucleus and enveloped by intranuclear microvesicles in the ring zone to form ODVs, which are finally embedded within a proteinaceous crystal matrix to form occlusion bodies (OBs) (8). When insect hosts orally consume OB-contaminated food, ODVs can initiate primary infection in midgut epithelial cells. Subsequently, BVs spread the infection from cell to cell and cause systemic infection in insect hosts. The anterograde transport of nucleocapsids within infected cells is crucial for BV morphogenesis and production and for viral pathogenicity.

Autographa californica multiple nucleopolyhedrovirus (AcMNPV) is the most extensively studied baculovirus and belongs to the genus *Alphabaculovirus*. In addition to cellular microtubules, actin cytoskeletons, and ESCRT-III proteins (9–11), some viral structural proteins encoded by AcMNPV have been found to participate in the anterograde transport of nucleocapsids. VP80 has been reported to interact with F-actin in the nuclei of infected cells to mediate the transport of nucleocapsids from the VS to the periphery of the nucleus (9, 12). Viral proteins that are essential for intranuclear microvesicle and ODV formation, including Ac93, Ac76, Ac75, Ac11, and Ac142, are also essential for the nuclear egress of nucleocapsids (13–18). In addition, two other proteins, Ac141 and Ac66, have also been found to be required for efficient nuclear egress of nucleocapsids (19, 20). For transport in the Cyt, baculovirus nucleocapsids have been shown to depend on the microtubule system, and Ac141 and the major capsid protein VP39 participate in this process by interacting with a motor protein of microtubules, namely, kinesin 1 (10, 21). When the nucleocapsids reach the plasma membrane, they bud from GP64-modified sites to gain envelopes and form mature BVs (22, 23). Therefore, GP64, as the BV-specific envelope protein, is essential for BV budding.

Based on phylogenetic evidence, the family *Baculoviridae* is subdivided into four genera: *Alphabaculovirus*, *Betabaculovirus*, *Gammabaculovirus*, and *Deltabaculovirus* (24). To date, BVs have not been found in gammabaculoviruses and deltabaculoviruses (25). One of the cytopathological differences between alphabaculoviruses and betabaculoviruses is that the nuclei of alphabaculovirus-infected cells remain intact during infection, while betabaculovirus infections generally induce an apparent breakdown of the NM during the early infection phase (8). Therefore, nucleocapsid egress from the NM is thought to be critical for *Alphabaculovirus* evolution. Moreover, although the BV morphogenesis of betabaculoviruses is completed in the hybrid cellular compartment, BV production by these viruses in cultured cells is very low (26); in contrast, the BV yields of alphabaculoviruses can be very high in cell cultures. Nucleocapsids use the microtubule system to cross the cytoplasmic space and bud from GP64-modified plasma membranes. However, little is known about the mechanism by which nucleocapsids cross the NM to reach the cytoplasm.

ac51 is one of the genes that are exclusively conserved in almost all sequenced

alphabaculoviruses, and the function of the gene in the viral life cycle remains unknown. To date, only a few studies have focused on the characterization of *ac51* and its orthologs. Proteomic analysis of AcMNPV BV and ODV components identified Ac51 as a component of AcMNPV BVs (27) but not ODVs (28). *ha39*, an *ac51* ortholog in Helicoverpa armigera nucleopolyhedrovirus (HearNPV), was transcribed at 3 h postinfection (hpi); the protein product (Ha39) was detected from 6 hpi to 72 hpi and is a structural protein of BVs, but not ODVs (29). However, proteomic analysis identified Ha39 from ODVs but not BVs (30). An *ac51* ortholog in Spodoptera litura nucleopolyhedrovirus (SpltNPV), namely, *sl39*, was transcribed at 6 hpi; the protein product (Sl39) was detected from 24 hpi to 72 hpi and is associated with both BVs and ODVs (31). In a comprehensive analysis of the knockout phenotypes of each gene of Bombyx mori nucleopolyhedrovirus (BmNPV), deletion of *bm40*, the *ac51* ortholog in BmNPV, resulted in a lethal phenotype (32). Mass spectrometric analysis showed that Bm40 is a component of ODVs (33).

A recent study published during the preparation of our manuscript reported that deletion of *bm40* resulted in the absence of infectious BV production and prevented ODV formation, but viral DNA replication and nucleocapsid assembly in the VS were not affected (34). Although both AcMNPV and BmNPV are group I alphabaculoviruses and share high DNA sequence identity, these viruses exhibit nonoverlapping host ranges (35). This phenomenon may be due to specific and adaptive virus-host interactions resulting from the ancient coevolution of baculoviruses and their hosts (36, 37). A study showed that the AcMNPV *p143*, *ie2*, and *p35* genes could not be replaced with the BmNPV orthologs in transient late gene expression assays, suggesting that host-specific factors may affect the mechanisms by which orthologous proteins function in different hosts (38). In addition, the virus-encoded helicases, namely, P143, from AcMNPV and BmNPV share approximately 96% sequence identity; however, AcMNPV P143 triggered rRNA degradation and apoptosis in AcMNPV-infected BmN cells, while BmNPV seems to have evolved a unique P143 to evade antiviral responses and allow replication in BmN cells (36, 39–41). Therefore, assessment of the role of Ac51 in the AcMNPV life cycle will also be valuable.

In this study, we performed a detailed investigation of the function of Ac51 in *Spodoptera frugiperda* cells by generating an *ac51* knockout AcMNPV. We analyzed the transcription of the *ac51* gene and the expression and localization of the Ac51 protein. The effects of *ac51* deletion on BV production, viral DNA replication, viral gene expression, and virion morphogenesis were evaluated. Our results demonstrate that *ac51* is not essential for AcMNPV replication, nucleocapsid assembly, and ODV formation, but deletion of the gene reduced the efficiency of the nuclear egress of nucleocapsids and resulted in a 1,000-fold decrease in BV production. Although Bm40 and Ac51 share nearly 94% sequence similarity and some results were consistent between them, some discrepancies remained; for example, Bm40 deletion prevented BV and ODV formation, while the *ac51* knockout AcMNPV produced a few infectious BVs and did not interrupt ODV formation. These discrepancies may help reveal the mechanisms by which these orthologous genes evolve and function and the differences between the AcMNPV/Sf9 and BmNPV/BmN cell systems.

RESULTS

Analysis of the transcription and expression of *ac51*. *ac51* has been classified as a delayed-early viral gene in the temporal transcription program of AcMNPV in *S. frugiperda* cells via DNA microarray experiments according to the classification criteria of Jiang et al's paper (42); however, deep sequencing of the 5′-capped transcription start sites of AcMNPV in *Trichoplusia ni* cells showed that *ac51* is transcribed from the canonical baculovirus late promoter TAAG (43). In the present study, we assessed the transcription pattern of *ac51* by reverse transcription (RT)-PCR in Sf9 cells. As shown in Fig. 1A, the RT-PCR results showed that *ac51* transcripts were detectable at 6 hpi and remained detectable up to 48 hpi. Meanwhile, the transcription patterns of the immediate-early gene *pe38*, the delayed-early gene *gp64*, and the late gene *vp39* were

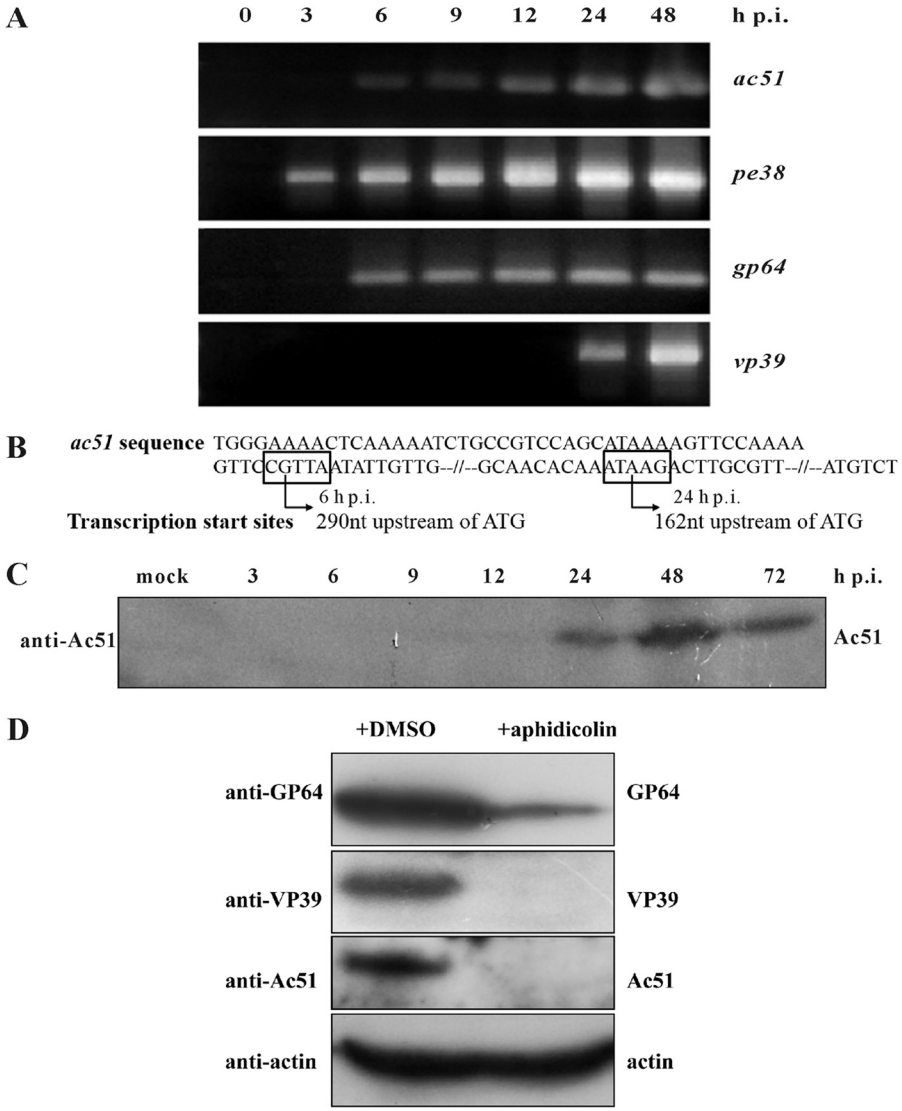

FIG 1 Analysis of the transcription and expression of *ac51* in Sf9 cells. (A) Transcription kinetics of *ac51* determined by RT-PCR. Total RNA was isolated from AcMNPV-infected Sf9 cells at the indicated time points and subjected to RT-PCR. *ac51*-, *pe38*-, *gp64*-, or *vp39*-specific primers were used to amplify the transcripts of *ac51*, *pe38*, *gp64*, and *vp39*, respectively. (B) Transcription start sites of *ac51*. Total cellular RNA was isolated from AcMNPV-infected Sf9 cells at 6 and 24 hpi and subjected to 5′ RACE analysis. The nucleotide sequence of the *ac51* promoter region is partially shown. The boxed sequences represent the promoter elements, and the arrows indicate the transcription start sites of *ac51*. (C) Temporal expression of Ac51. Sf9 cells were infected with vAcWT at an MOI of 10 $TCID_{50}$/cell, collected at the indicated time points, and subjected to Western blot analysis. Ac51 was detected with an anti-Ac51 antibody. (D) Ac51 expression requires viral DNA replication. Sf9 cells were infected with vAcWT at an MOI of 5 $TCID_{50}$/cell, and the DNA synthesis inhibitor aphidicolin (dissolved in DMSO) at 5 μg/ml or DMSO only was added to the cells during infection and maintained thereafter. The cells were collected at 24 hpi and subjected to Western blot analysis. An anti-GP64 antibody, anti-VP39 antibody, anti-Ac51 antibody, or anti-actin antibody was used as the primary antibody.

also determined and are shown in Fig. 1A. To map the transcription start site of *ac51*, rapid amplification of 5′ cDNA ends (5′ RACE) analysis was conducted using total RNA isolated from AcMNPV-infected cells at 6 or 24 hpi. DNA sequencing showed that the transcription of *ac51* was initiated from the G (nucleotide [nt] −290) of an atypical promoter element, CGTTA, at 6 hpi and from the first A (nt −162) of the typical late promoter motif, TAAG, at 24 hpi (Fig. 1B). The latter motif is identical to that observed in the transcription of this gene in *T. ni* cells.

To determine the temporal expression profile of Ac51, wild-type AcMNPV-infected Sf9 cells were collected at the indicated time points and subjected to Western blot

analysis using a rabbit polyclonal antibody against Ac51. As shown in Fig. 1C, an immunoreactive band of approximately 37 kDa, which is similar to the predicted molecular mass of Ac51, was detected from 24 hpi to 72 hpi.

Since baculovirus late genes require viral DNA replication for expression, Ac51 expression was examined in the presence of aphidicolin, a DNA synthesis inhibitor, to determine whether it is an early or late viral gene. As shown in Fig. 1D, in the presence of aphidicolin, Ac51 was not detected, while the product of the early and late gene *gp64* was still detected and the product of the late gene *vp39* was not detected as expected. Therefore, *ac51* can be designated a late viral gene.

***ac51* deletion substantially reduced BV production in Sf9 cells.** To investigate the role of *ac51* in the AcMNPV life cycle, an *ac51* knockout AcMNPV bacmid (bAc51KO) was constructed based on the bacmid bMON14272 via λ Red homologous recombination. According to a previous study and as shown in Fig. 2A, the interval between *ac51* and its upstream *lef8* gene or its downstream *ac52* gene is 26 bp or 202 bp, respectively (44). Transcriptional analysis of AcMNPV in *T. ni* cells showed that *lef8* initiates transcription in the reverse direction at nt 43175 (Fig. 2A, arrow), while the polyadenylation site of *ac52* is at nt 43693, which is within the coding region of *ac51* (Fig. 2A, arrowhead) (43). Thus, to avoid any modulation of adjacent gene expression, the N-terminal 125-bp fragment (nt 43514 to 43638) of *ac51* was replaced with a chloramphenicol resistance gene (*CmR*) cassette in bAc51KO (Fig. 2A).

To examine the effect of *ac51* deletion on OB morphogenesis and to facilitate observation of the progress of viral infection, an AcMNPV polyhedrin (*polh*) gene under its native promoter and an enhanced green fluorescent protein (*egfp*) gene under the AcMNPV *ie1* promoter were inserted into the *polh* gene locus of bAc51KO, and the new construct was named vAc51KO (Fig. 2A). Meanwhile, an *ac51* repair virus (vAc51REP) was generated by inserting an *ac51* gene cassette under its own promoter, together with the *polh* and *egfp* genes, into the *polh* locus of bAc51KO to confirm the phenotype resulting from the deletion of *ac51*. vAcWT was constructed by inserting the *polh* and *egfp* genes into the *polh* locus of bMON14272 to serve as a wild-type AcMNPV control (Fig. 2A).

Sf9 cells were transfected with 1.0 μg of vAc51KO, vAc51REP, or vAcWT bacmid DNA and monitored with a fluorescence microscope. No obvious differences in the numbers of fluorescent cells were observed among the viruses at 24 h posttransfection (hpt), indicating relatively equal frequencies of transfection (Fig. 2B). By 96 hpt, almost all of the vAc51REP- or vAcWT-transfected cells exhibited fluorescence. However, the number of fluorescent cells observed with vAc51KO transfection increased slightly from 24 to 96 hpt, suggesting that vAc51KO was capable of generating infectious BVs, but not as efficiently as vAc51REP and vAcWT (Fig. 2B). Light microscopy revealed that OBs were formed in vAc51KO-transfected cells, indicating that vAc51KO progressed into the very late stage of infection. A plaque assay showed that vAcWT and vAc51REP produced viral plaques with comparable diameters, with no significant difference ($P = 0.80$). However, the diameters of the vAc51KO plaques were reduced to approximately 20% of those of the vAcWT plaques ($P < 0.001$) (Fig. 2C).

Viral growth curve analyses showed that vAc51REP and vAcWT had similar growth trends. Infectious BVs could be detected, and equivalent amounts ($P = 1.00$) were observed in the supernatants of vAc51REP- or vAcWT-transfected cells at 24 hpt. By 96 hpt, the BV levels of vAc51REP and vAcWT were comparable ($P = 0.10$), indicating that vAc51REP replicated as efficiently as vAcWT. However, infectious BVs were not detected in the supernatants of vAc51KO-transfected cells until 48 hpt (Fig. 2D), at which time the BV yields were nearly 280-fold lower than those of vAcWT-transfected cells ($P < 0.01$). By 96 hpt, an up to 1,000-fold ($P < 0.01$) reduction was observed (Fig. 2D), corresponding to a reduction by approximately 99.9%.

To analyze the effect of *ac51* deletion on viral replication under conditions of BV infection, Sf9 cells were infected with vAc51KO, vAc51REP, or vAcWT at a multiplicity of infection (MOI) of 0.2 50% tissue culture infective dose ($TCID_{50}$)/cell, and BV production

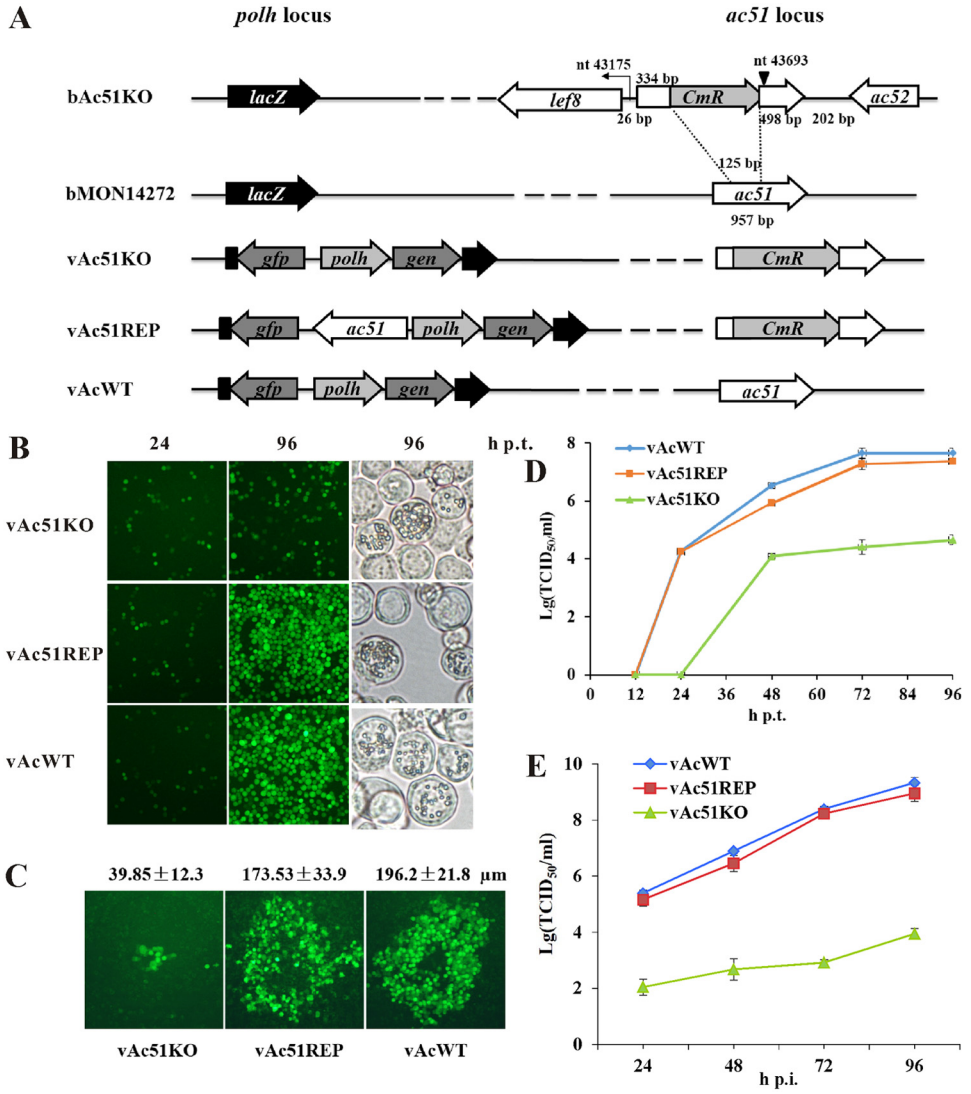

FIG 2 Schematic diagram of recombinant virus construction and replication analysis of these viruses in Sf9 cells. (A) Schematic diagram of recombinant viruses. bAc51KO was constructed by replacing a 125-bp fragment of *ac51* in bMON14272 with a *CmR* cassette via homologous recombination in *E. coli*. The interval between *ac51* and *lef8* or *ac52* is 26 bp or 202 bp, respectively. The transcription start site of *lef8* is at nt 43175, and the polyadenylation site of *ac52* is at nt 43693. vAc51KO was generated by inserting the *polh* and *egfp* genes into the *polh* locus of bAc51KO via Tn*7*-mediated transposition. The preserved regions at the 3′ and 5′ ends of the *ac51* ORF are indicated. vAc51REP was constructed by transposing the *ac51* ORF under its native promoter into the *polh* locus of bAc51KO, together with the *polh* and *egfp* genes. vAcWT was generated by transposing the *polh* and *egfp* genes into the *polh* locus of bMON14272. *gen*, gentamicin. (B) Fluorescence microscopy of cells transfected with vAc51KO, vAc51REP, or vAcWT bacmid DNA. Light microscopy images show the formation of OBs. (C) Plaque assays of vAc51KO-, vAc51REP-, or vAcWT-transfected cells. Viral plaques were visualized using a fluorescence microscope at 120 hpt. Seventeen different well-isolated plaques of each virus were selected, and the diameters of the plaques were measured. (D) Viral growth curves generated from bacmid-transfected Sf9 cells. Infectious BV production in the supernatants of vAc51KO-, vAc51REP-, or vAcWT-transfected cells was determined by an endpoint dilution assay at the indicated time points. (E) Viral growth curves generated from virus-infected Sf9 cells. Sf9 cells were infected with vAc51KO, vAc51REP, or vAcWT at an MOI of 0.2 $TCID_{50}$/cell. BV production at each time point was determined by an endpoint dilution assay. The values at each time point in panels D and E represent the averages of three independent experiments. The error bars indicate the standard deviations.

at each time point was determined. The results of this time course analysis revealed that BV titers of both vAc51REP and vAcWT were comparable at each time point and reached nearly 10^9 $TCID_{50}$/cell at 96 hpi (Fig. 2E). In contrast, the BV titer of vAc51KO increased slightly over time and was only 8×10^3 $TCID_{50}$/cell at 96 hpi (Fig. 2E), which is 10^5 lower than the BV titer of vAcWT. Taken together, these results demonstrate that

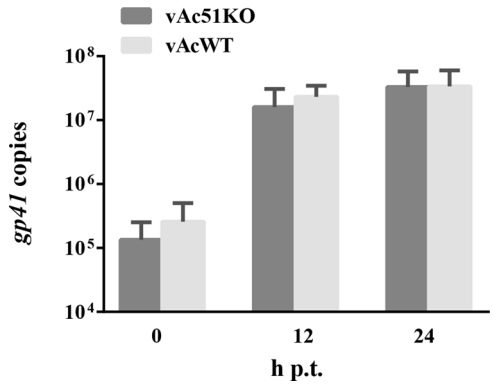

FIG 3 Analysis of viral DNA replication. Sf9 cells were transfected with vAc51REP or vAc51KO bacmid DNA. At the designated time points, total intracellular DNA was isolated and digested with DpnI to eliminate the bacmid DNA introduced during transfection. AcMNPV *gp41* copy numbers were determined by qPCR to represent the genome copies. The results represent the averages of three independent assays. The error bars indicate standard deviations.

ac51 is not essential for viral replication in cultured cells but is required for efficient BV production.

***ac51* is not required for viral DNA replication.** Reduction of BV production by *ac51* deletion may be a consequence of a defect in viral DNA replication or viral gene expression. Thus, we first assessed the effect of *ac51* deletion on viral DNA replication within 24 hpt, when the secondary infection of BVs is not supposed to occur. Sf9 cells transfected with vAc51REP or vAc51KO bacmid DNA were collected at 0, 12, and 24 hpt, and total cellular DNA was extracted. AcMNPV *gp41* gene copies were used to represent the viral genome copies, as previously described (45), and the copy numbers were determined by quantitative real-time PCR (qPCR). As shown in Fig. 3, the genomic DNA content of vAc51REP or vAc51KO increased from 12 to 24 hpt, and both exhibited levels at these time points significantly higher than those at 0 hpt. Student's *t* test showed no significant differences between the genomic DNA contents of vAc51REP- and vAc51KO-transfected cells at any of the studied time points ($P = 0.48$, 0.52, and 0.98 at 0, 12, and 24 hpt, respectively), indicating that *ac51* is not required for viral DNA replication.

***ac51* deletion does not affect early and late viral gene expression.** Subsequently, we investigated the effects of *ac51* deletion on viral gene transcription and viral protein synthesis during the viral life cycle. Sf9 cells transfected with vAc51KO or vAcWT bacmid DNA were collected at 24 hpt, and total cellular RNA was extracted. Six viral genes were selected to represent the immediate-early (*ie1*), delayed-early (*lef6*, *lef9*, and *gp64*), and late (*vp39* and *p6.9*) viral genes. The transcript levels of these genes were determined by RT-qPCR with corresponding primers (shown in Table 1). The results showed that the transcript levels of all the selected genes did not significantly differ between vAc51KO- and vAcWT-transfected cells (Fig. 4A), suggesting that both early and late viral transcription were not affected by *ac51* deletion.

Furthermore, Western blot analysis was performed to assess the protein levels of GP64, VP39, and P6.9, which are all crucial for BV morphogenesis (23, 46, 47). Sf9 cells transfected with vAc51KO or vAcWT bacmid DNA were collected at 12, 18, and 24 hpt. Production of the viral early protein GP64 and viral late proteins VP39 and P6.9 was analyzed with the corresponding antibodies. Actin was detected to indicate comparable sample loading. As shown in Fig. 4B, in both vAc51KO- and vAcWT-transfected cells, GP64 was first detected at 12 hpt, while VP39 and P6.9 were first detected at 18 hpt, and the expression levels of all the genes increased upon infection. No clear difference was found between the protein expression patterns of vAc51KO- and vAcWT-transfected cells. A nonspecific band (indicated by the asterisk) was detected with an antibody against P6.9, and this band could also be used as an internal control. Together, these results suggest that *ac51* is not required for early and late viral gene expression.

TABLE 1 Primers used in this study and their sequences

Primer[a]	Sequence (5′→3′)
515	TGTAAAACGTCCTACAACTATGAACA
513	TTATGTGTAAGATTTTAAAGCGTTT
pe385	ATTAATTTTAAATTTGAGTG
pe383	ATTTTCAAACCCAAAATTAA
gp645	CGCTGGCATCTTTCCAACTGT
gp643	TTCATCGAGACGGCGTGAGTA
vp395	TGAGAGTTAATCGCTGCATTTTCGC
vp393	CTCTTGGTATAAAGTCGTTGCGC
51L5	GATTTTAATAAAAAATGCGCGTTTAGTGCTTAGTAATAGTG TCAAAAAGCTTCGAATAAATACCTGTGA
51L3	CTGGGTTGTTTATATCCGACTTGTCGGGTTTATT AGTAAAAATATTGACCAACCAGCAATAGACATAAG
51P5	GAGCTCCGCGATTGATGTGCTTCTCTTG
51rep5	GGTACCATGTCTAAACGTGTTCGTGAACG
51rep3	GGATCCTTATGTGTAAGATTTTAAAGCGTTT
51sp1	TTGTAAAAAGACCGTAATCAATGGA
51sp2	ATTAAAATCAACACGTTACGCACCG
gp41F	CGTAGTGGTAGTAATCGCCGC
gp41R	AGTCGAGTCGCGTCGCTTT
ie1F	TTGTGATAAACAACCCAACGA
ie1R	GTTAACGAGTTGACGCTTGC
lef6F	TAGATTCTCCTCGCTTGG
lef6R	ATTTCGCCATCTTCTAAATT
gp64F	ATCAAACGCTCGTCCACC
gp64R	GGGAGACACTGCCACCAAA
vp39F	TTGCGCAACGACTTTATACC
vp39R	TAGACGGCTATTCCTCCACC
p6.9F	GGCGACCTGTCGATGAA
p6.9R	CGCAGAAGCTCGGGTTA
18S rRNAF	TACCGATTGAATGATTTAGTGAGG
18S rRNAR	TACGGAAACCTTGTTACGACTTT
gfpF	GAATTCATGGGCAAAGGAGAAGAACTTTTCACTG
gfpR	TCTAGATTATTTGTATAGTTCATCCATGCCATG
actinF	AGTCGACAATGGCTCCGGCATG
actinR	GCGTAACCTTCGTAGATGGGGAC

[a]F, forward primer; R, reverse primer.

Ac51 is distributed in both the nuclei and cytoplasm of infected cells and is a nucleocapsid protein of BVs. To further explore Ac51 function, an antibody was raised against AcMNPV Ac51, and the localization of Ac51 in infected cells and virions was analyzed. Sf9 cells infected with vAcWT were subjected to an immunofluorescence assay at 24, 48, and 72 hpi. The subcellular localization of Ac51 was investigated using the anti-Ac51 antibody. Hoechst 33342, which can stain DNA, was used to visualize the nucleus. Uninfected Sf9 cells were also stained with the anti-Ac51 antibody as a negative control. As shown in Fig. 5, at 24 hpi, Ac51 was distributed in the nucleus, exhibiting a ring pattern in the ring zone and a dot distribution pattern in the VS, and also in the cytoplasm. As viral infection persisted, Ac51 fluorescence became more intense and showed the same localization pattern at 48 hpt. This localization pattern was maintained until 72 hpi (Fig. 5).

As *ac51* deletion affected BV production, it was necessary to determine whether Ac51 is associated with virions. BVs and ODVs were purified from vAcWT-infected Sf9 cells, and the BVs were further biochemically fractionated into nucleocapsid (NC) and envelope (E) fractions. These virions and fractions were subjected to Western blot analysis, and the localization of Ac51 was analyzed. As shown in Fig. 6A, Ac51 was localized in both BVs and ODVs and was associated with the nucleocapsid fraction of BVs. The localization of the BV envelope protein GP64 and the nucleocapsid protein VP39 was analyzed to confirm the efficiency of fractionation. Both GP64 and VP39 were detected in the expected fractions. These results demonstrate that Ac51 is associated with both BVs and ODVs and is a nucleocapsid protein of BVs.

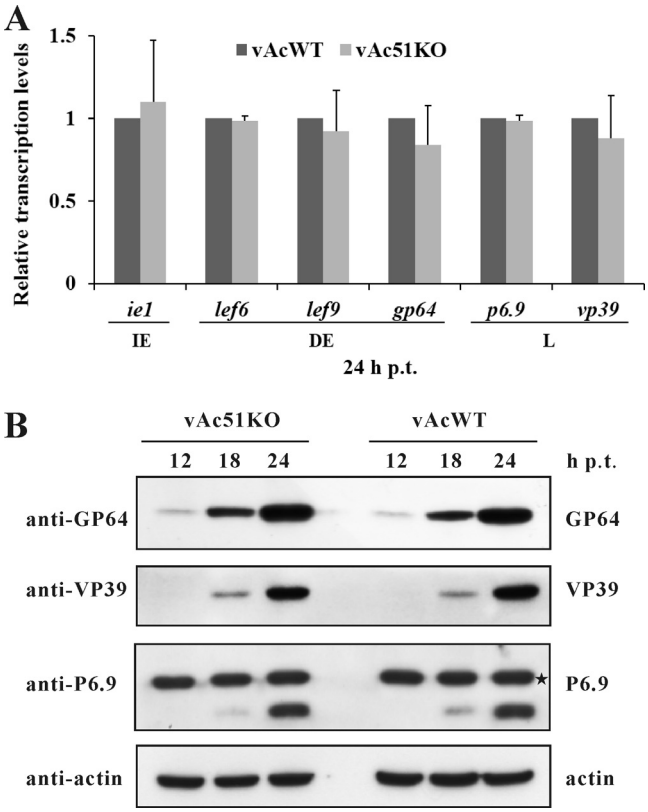

FIG 4 Analysis of viral gene expression. (A) RT-qPCR analyses of the transcription of selected viral genes at 24 hpt. Sf9 cells were transfected with vAc51KO or vAcWT bacmid DNA, and the transcript levels of the indicated genes were measured by RT-qPCR. The level of each gene was normalized to that of the host 18S rRNA. The ordinate shows the percentage of each gene level in the vAc51KO-transfected cells relative to the level in the vAcWT-transfected cells. The experiment was performed four times, and the error bars represent standard deviations. IE, immediate-early gene; DE, delayed-early gene; L, late gene. (B) Western blot analysis of the temporal expression of GP64, VP39, and P6.9. Sf9 cells transfected with vAc51KO or vAcWT bacmid DNA were scraped at 12, 18, and 24 hpt and subjected to Western blot analysis. An anti-GP64, anti-VP39, or anti-P6.9 antibody was used as the primary antibody. Actin was detected with an anti-actin antibody as a loading control.

Immunoelectron microscopy (IEM) was used to further confirm the association of Ac51 with virions. As shown in Fig. 6B to D, colloidal-gold-labeled Ac51 was distributed specifically on the nucleocapsids in both the interspaces of the VS (Fig. 6B and C) and the ring zone (Fig. 6D), indicating that Ac51 is a nucleocapsid protein.

***ac51* deletion does not affect nucleocapsid assembly.** Since Ac51 is a virion structural protein, we investigated the effect of *ac51* deletion on virion assembly by transmission electron microscopy (TEM). Sf9 cells transfected with vAc51KO or vAcWT bacmid DNA were subjected to TEM. In vAc51KO-transfected cells, the VS was formed in the centers of the nuclei at 24 hpt (Fig. 7E), and abundant rod-shaped electron-dense nucleocapsids were present in the interspaces of the electron-dense mats of the VS at 48 hpt (Fig. 7F). These observations were similar to those in vAcWT-transfected cells (Fig. 7A and B). At 72 hpt, mature ODVs containing single or multiple nucleocapsids prior to occlusion (Fig. 7G) and polyhedra (P) containing ODVs (Fig. 7H) were present in the ring zone, which was similar to the phenomenon observed in vAcWT-transfected cells (Fig. 7C and D). These results indicate that *ac51* deletion does not interrupt nucleocapsid assembly or ODV and OB formation.

***ac51* is required for efficient nuclear egress of nucleocapsids to form BVs.** The last step of BV morphogenesis is intracellular transport of nucleocapsids from the nucleus to the cytoplasmic membrane (CM), where the nucleocapsids bud to form mature BVs. As a nucleocapsid protein, Ac51 is possibly involved in this process.

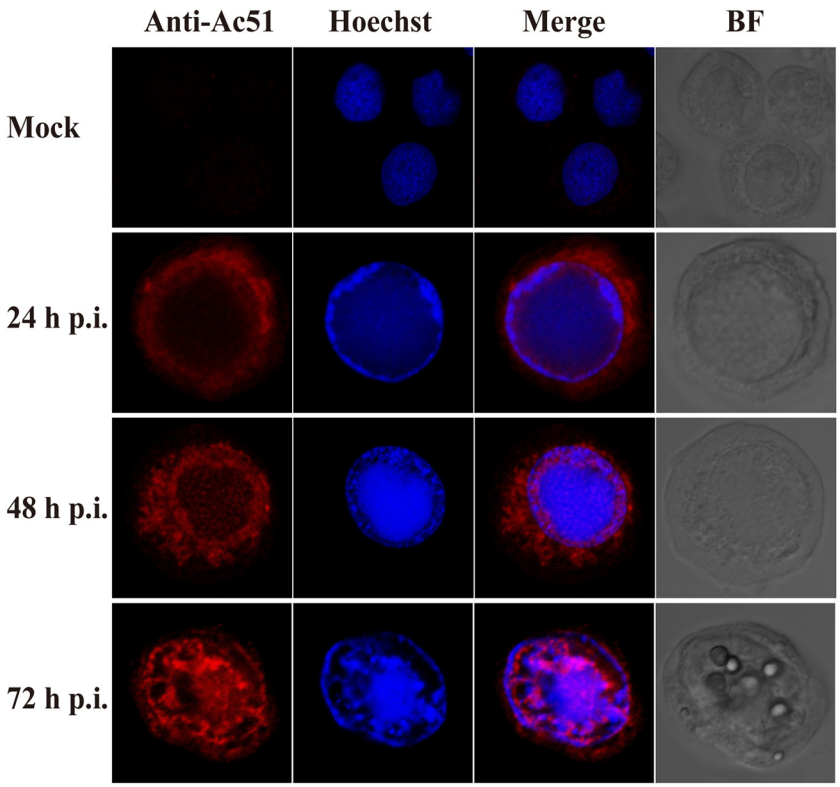

FIG 5 Localization of Ac51 in infected Sf9 cells. Sf9 cells were infected with vAcWT at an MOI of 5 $TCID_{50}$/cell. At the indicated time points, the cells were probed with an antibody against Ac51, incubated with an Alexa Fluor 555-conjugated donkey anti-rabbit secondary antibody, and subsequently stained with Hoechst 33342. Subcellular localization of Ac51 was then examined with a Zeiss7 Duo NLO confocal microscope. BF, bright field.

Therefore, we first examined the number of BVs released into the cell culture supernatants during a viral life cycle. The BVs were purified from the culture supernatants of cells transfected with vAc51KO or vAcWT bacmid DNA at 24 hpt and subjected to Western blot analysis. The levels of the major capsid protein VP39 and the BV envelope protein GP64 in the supernatants were used to represent BV levels. As shown in Fig. 8A, the levels of intracellular GP64 or VP39 in vAc51KO- and vAcWT-transfected cells were comparable, suggesting similar amounts of synthesized viral proteins in these cells. However, the levels of both GP64 and VP39 in the culture supernatants of vAc51KO-transfected cells were markedly lower than the levels of these proteins in vAcWT-transfected cells (Fig. 8A), indicating that vAc51KO produced substantially fewer BVs than vAcWT in a single life cycle. This result indicates that Ac51 is required for anterograde transport of nucleocapsids to form BVs.

Subsequently, TEM was performed to further identify the step in which Ac51 is involved during anterograde transport of nucleocapsids. We found that egressing nucleocapsids (including those penetrating the NM, transiting the Cyt, or budding from the CM) were frequently observed in vAcWT-transfected cells but only occasionally observed in vAc51KO-transfected cells (Fig. 8B). Thus, a statistical analysis was conducted according to reported methods used in baculovirus (19, 20) and herpesvirus (48–50) studies. The numbers of nucleocapsids in the nuclei and egressing nucleocapsids in vAc51KO- or vAcWT-transfected cells were determined and compared. As shown in Table 2 and Fig. 9A, the numbers of nucleocapsids observed in the nuclei of vAcWT- or vAc51KO-transfected cells were comparable, and no significant difference was found in the mean numbers of nucleocapsids at 36, 48, or 72 hpt ($P = 0.78$, 0.62, and 0.95 at 36, 48, and 72 hpt, respectively), suggesting that nucleocapsid assembly and production were not affected by *ac51* deletion. However, the number of egressing nucleo-

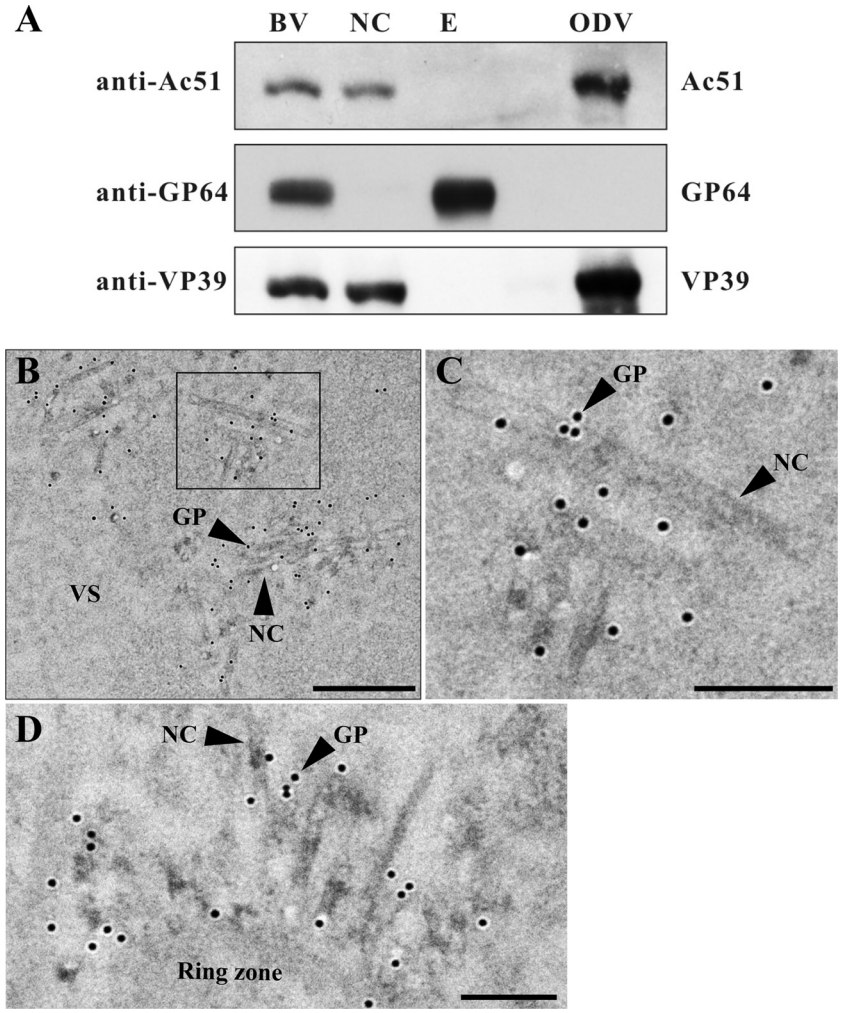

FIG 6 Localization of Ac51 in virions. (A) BV particles were purified from the culture supernatants of vAcWT-infected Sf9 cells and fractionated into nucleocapsid and envelope fractions. ODVs were purified from the vAcWT-infected Sf9 cells. The fractions were then subjected to Western blot analysis. Ac51, GP64, and VP39 were detected with the corresponding antibodies as indicated. NC, nucleocapsid of BVs; E, envelope of BVs. (B to D) Sf9 cells infected with vAcWT were subjected to IEM at 72 hpi. The anti-Ac51 antibody was used as the primary antibody, and a colloidal gold nanoparticle-conjugated donkey anti-rabbit antibody was used as the secondary antibody. (B and C) Distributions of colloidal gold nanoparticles in the VS (B) and ring zone (C) of infected cells. The boxed region in panel B is magnified in panel C. NC, nucleocapsids; GP, gold particles. Bars, 500 nm (B) and 200 nm (C and D).

capsids of vAc51KO was much lower than that of vAcWT at each time point (Table 2). Compared with vAcWT, the mean number of egressing nucleocapsids decreased by approximately 1.7-, 3.2-, and 4.5-fold at 36, 48, and 72 hpt, respectively, and the values were statistically significant at 48 and 72 hpt ($P \leq 0.001$ at 48 and 72 hpt) (Fig. 9B), suggesting a role for Ac51 in the process of nucleocapsid egress from the nucleus.

We further analyzed the number of nucleocapsids crossing the NM, transiting the Cyt, or budding from the CM at each time point. As shown in Fig. 9, substantially less nucleocapsid egress was observed in vAc51KO- or vAcWT-transfected cells at 36 hpt (Fig. 9C) than at 48 or 72 hpt (Fig. 9D and E), and among the egressing nucleocapsids at 36 hpt, most (nearly 68% in vAc51KO and 59% in vAcWT) were crossing the NM (Fig. 9C). These results suggested that nucleocapsid egress from the nucleus was in the initial stage at 36 hpt, which may explain why no significant difference was observed in the numbers of egressing nucleocapsids between vAc51KO and vAcWT at 36 hpt. At 48 hpt, most (nearly 84%) of the egressing nucleocapsids of vAcWT were transiting the Cyt and budding, and approximately 16% were crossing the NM, but a large number of

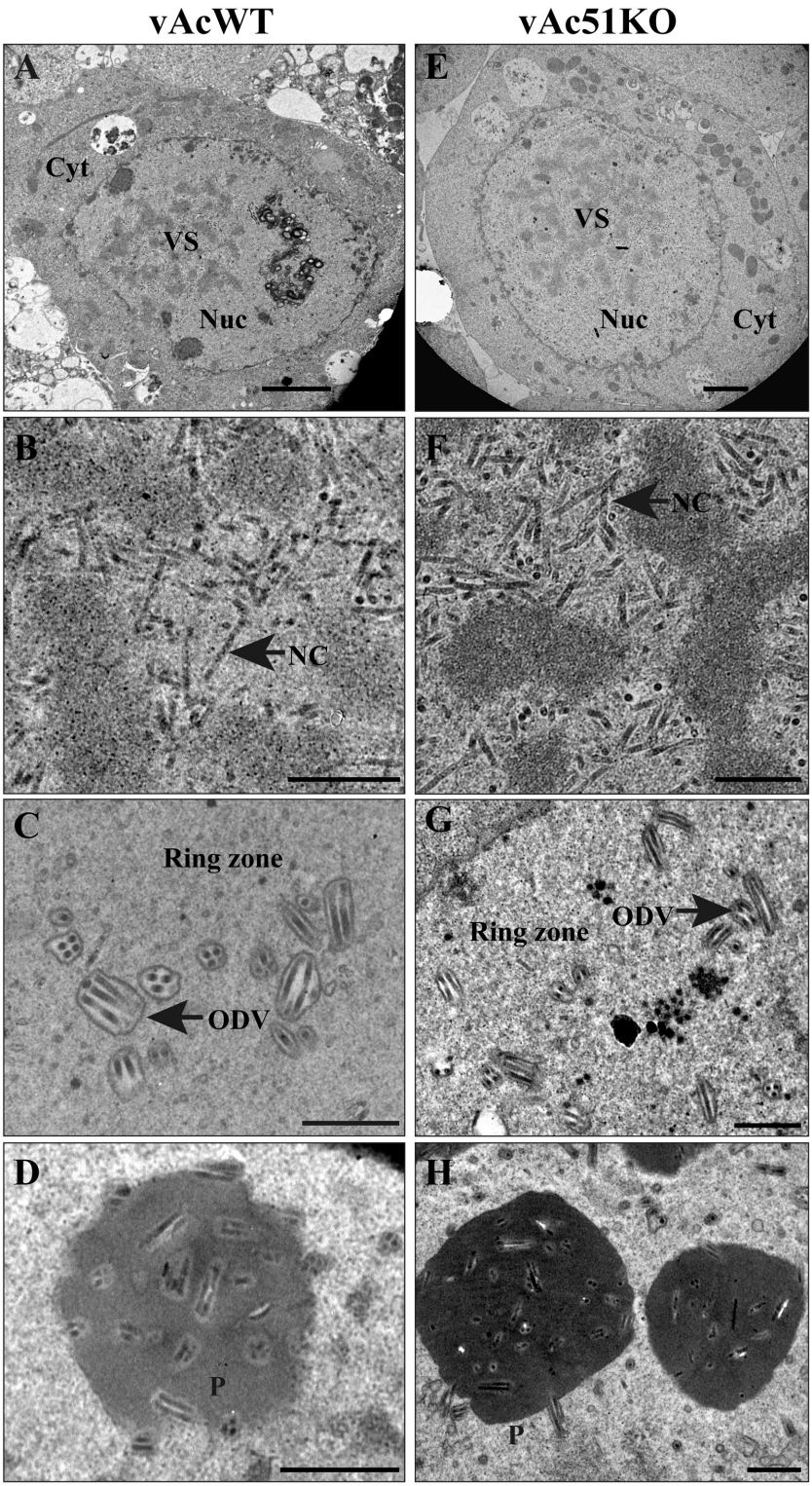

FIG 7 Analysis of viral morphogenesis in vAc51KO-infected cells by TEM. Sf9 cells were transfected with vAc51KO or vAcWT bacmid DNA; collected at 24, 48, and 72 hpt; and prepared for TEM. (A to D) Cells transfected with vAcWT bacmid DNA. (E to H) Cells transfected with vAc51KO bacmid DNA. (A and E) Cell with a typical VS at 24 hpt. (B and F) Rod-shaped electron-dense nucleocapsids (NC) in the VS at 48 hpt. (C and G) Multiple enveloped mature ODVs, indicated by arrows, at 72 hpt. (D and H) Polyhedra (P) with embedded ODVs at 72 hpt. Bars, 2 μm (A and E) and 500 nm (B to D and F to H). Nuc, nucleus; Cyt, cytoplasm.

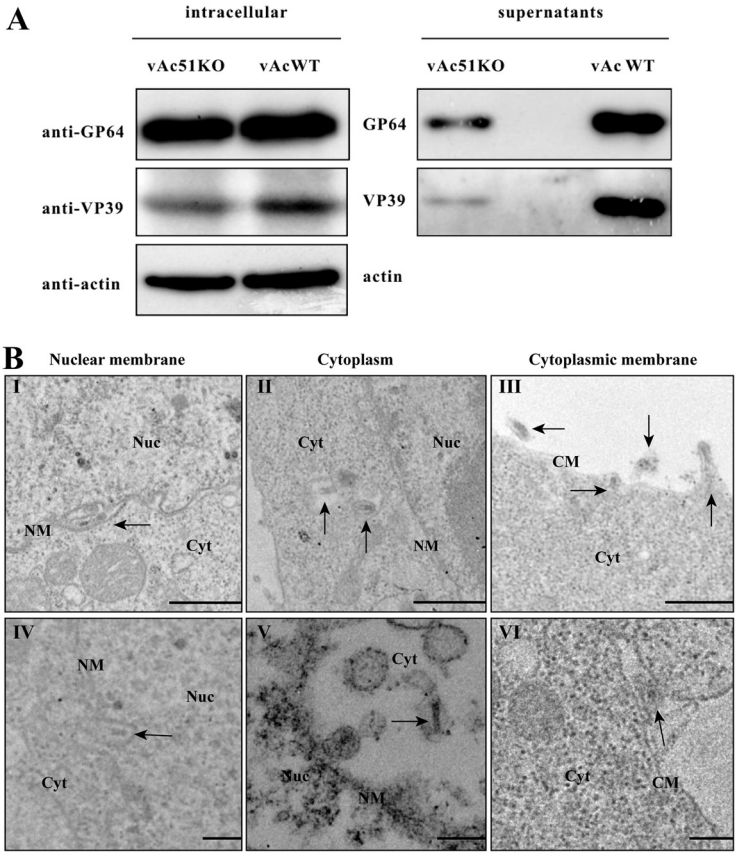

FIG 8 Effects of *ac51* deletion on nucleocapsid egress and BV formation. (A) Western blot analysis of total BV production in the culture supernatants of vAc51KO- or vAcWT-infected cells. Sf9 cells were transfected with vAc51KO or vAcWT bacmid DNA. At 24 hpt, BVs were purified from culture supernatants and subjected to Western blot analysis, together with the cell lysate. GP64 and VP39 were used to represent BVs in the supernatants, and the expression levels of these proteins in the cells were also determined. An anti-actin antibody was used to detect actin, which served as the loading control. (B) Egressing nucleocapsids, indicated by arrows, were observed in vAcWT-infected (I to III) or vAc51KO-infected (IV to VI) cells. (I and IV) Nucleocapsids penetrating the nuclear membrane (NM). (II and V) Nucleocapsids transiting the cytoplasm (Cyt). (III and VI) Nucleocapsids budding from the cytoplasmic membrane (CM). Nuc, nucleus. Bars, 500 nm.

egressing nucleocapsids of vAc51KO (nearly 45%) were crossing the NM (Fig. 9D). In addition, the mean numbers of nucleocapsids transiting the Cyt or budding between vAc51KO and vAcWT were statistically significant ($P = 0.02$ and 0.0003, respectively) (Fig. 9D), suggesting that some challenges may be associated with an efficient exit from the nucleus for nucleocapsids of vAc51KO. The phenotype of vAcWT at 48 hpt persisted

TABLE 2 Numbers of nucleocapsids in the nuclei of and in the process of budding from 10 vAcWT-transfected Sf9 cells and 10 vAc51KO-transfected Sf9 cells at 36, 48, and 72 hpt

Time point at which cells were observed (hpt)	No. of nucleocapsids at the indicated locations in cells transfected with:			
	vAcWT		vAc51KO	
	Nucleus	Budding[a]	Nucleus	Budding[a]
36	1,949	32	1,879	19
48	2,373	177	2,553	55
72	3,058	196	2,969	44
Total no. of nucleocapsids	7,380	405	7,401	118

[a]The total number of budding nucleocapsids comprises those penetrating the nuclear membrane, transiting the cytoplasm, and budding from the cytoplasmic membrane.

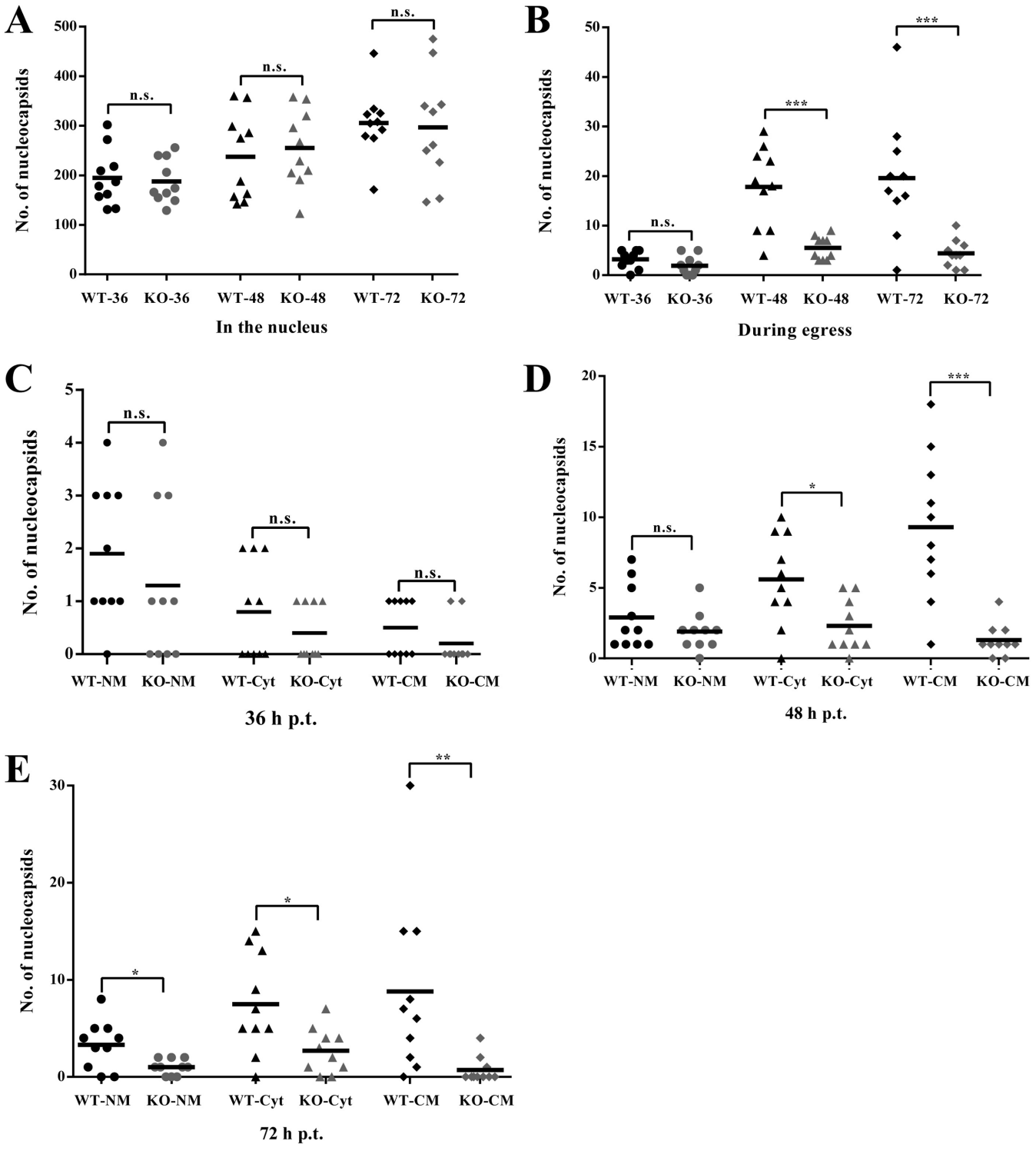

FIG 9 Numbers of nucleocapsids in the nucleus and egressing nucleocapsids in vAc51KO- or vAcWT-infected Sf9 cells. Sf9 cells transfected with vAc51KO or vAcWT bacmid DNA were subjected to TEM at 36, 48, and 72 hpt. Ten vAc51KO-transfected cells and 10 vAcWT-transfected cells from each time point were observed, and the nucleocapsids in the nucleus and egressing nucleocapsids in a whole-cell section of each cell were counted. The egressing nucleocapsids included those crossing the nuclear membrane (NM), transiting the cytoplasm (Cyt), and budding from the plasma membrane (CM). The horizontal bars indicate the mean number of nucleocapsids for each condition. The *P* values were calculated using the Mann-Whitney test. n.s., no significance; *, $P \leq 0.05$; **, $P \leq 0.01$; ***, $P \leq 0.001$. (A) Number of nucleocapsids in the nucleus of each of the 10 cells for each condition. (B) Number of egressing nucleocapsids in each of the 10 cells for each condition. (C to E) Numbers of nucleocapsids crossing the NM, transiting the Cyt, and budding from the CM in each of the 10 cells for each virus at 36 hpt (C), 48 hpt (D), and 72 hpt (E). KO, vAc51KO; WT, vAcWT. The numbers 36, 48, and 72 are the time points.

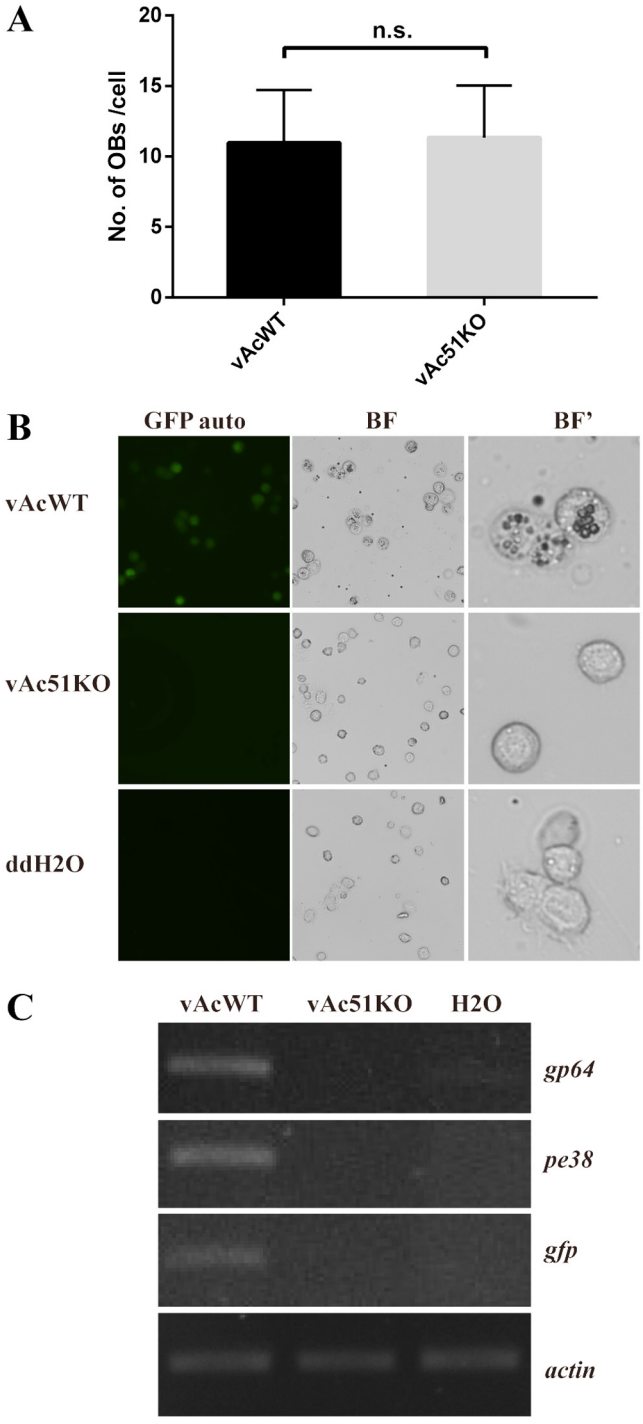

FIG 10 Effect of *ac51* deletion on AcMNPV infection *in vivo*. (A) OB production in infected Sf9 cells. Sf9 cells were transfected with bacmid DNA of vAc51KO or vAcWT. The OBs in a cell were counted, and a total of 100 cells were counted for each condition. n.s., no significance. (B) Effect of *ac51* deletion on systemic infection of AcMNPV. Hemolymph of vAcWT-infected, vAc51KO-infected, or H_2O-treated *S. exigua* larvae was collected 5 days after oral infection, dropped on a slide, and examined with a fluorescence microscope. Cells with GFP fluorescence were indicative of viral infection. BF, bright field. Column BF′ shows magnified fields of hemocytes. (C) Effect of *ac51* deletion on the primary infection of AcMNPV by RT-PCR. *S. exigua* larvae were treated with H_2O or OBs of vAcWT or vAc51KO. Total RNA of the larva guts was extracted, and RT-PCR was performed to detect the transcripts of the *pe38*, *gp64*, *gfp*, and *actin* genes.

TABLE 3 Infectivity of vAc51KO and vAcWT in third-instar *S. exigua* larvae

Administration condition	No. of treated larvae (Rep. 1/Rep. 2/Rep. 3)[a]	No. of liquefied larvae			No. of pupated larvae		
		Rep. 1	Rep. 2	Rep. 3	Rep. 1	Rep. 2	Rep. 3
vAcWT	15/15/15	15	15	15	0	0	0
vAc51KO	15/13/15	0	0	0	15	13	15
ddH_2O[b]	14/13/14	0	0	0	14	13	14

[a]Sixteen larvae were treated for each condition in each replicate (Rep.), but those that were dead with the whole body being black for unknown reasons within 3 days were excluded.
[b]ddH_2O, double-distilled H_2O.

until 72 hpt (Fig. 9E). The proportion of egressing nucleocapsids of vAc51KO transiting the Cyt and budding increased to nearly 77% at 72 hpt, but the mean number of egressing nucleocapsids under each condition was still significantly lower than that observed for vAcWT ($P = 0.03$, 0.02, and 0.002, respectively) (Fig. 9E). Taken together, our results indicate that *ac51* is not required for the assembly and production of nucleocapsids, but they suggest a role for Ac51 in the efficient egress of nucleocapsids from the nucleus to the Cyt.

***ac51* is essential for the virulence of AcMNPV in *Spodoptera exigua*.** Since ODVs and ODV-containing polyhedra were observed by TEM in vAc51KO-infected cells, we further determined whether *ac51* deletion affected the virulence of AcMNPV *in vivo*. OB production in Sf9 cells transfected with bacmid DNA of vAc51KO or vAcWT was first determined. The results showed that the average number of OBs in each vAc51KO-infected cell was comparable to that in each vAcWT-infected cell (Fig. 10A). Then, OBs purified from vAcWT- or vAc51KO-infected Sf9 cells were administered to newly molted 3rd-instar *Spodoptera exigua* larvae at a dose of 4×10^4 OBs/larva. As shown in Table 3, infection with OBs of vAcWT resulted in 100% liquification of *S. exigua* in three independent cohorts, while vAc51KO-infected *S. exigua* larvae all pupated. Noninfected *S. exigua* larvae were used as a negative control and showed a 100% survival rate. In a separate assay, the hemolymph of vAc51KO-infected, vAcWT-infected, or uninfected *S. exigua* larvae was collected 5 days after oral infection and observed with a fluorescence microscope. As shown in Fig. 10B, the hemocytes from vAcWT-infected larvae showed green fluorescence and contained OBs, which were indicative of viral infection. However, the hemocytes from vAc51KO-infected larvae showed no fluorescence and contained no OBs, similar to the uninfected larvae (Fig. 10B), indicating that vAc51KO was not able to establish systemic infection.

To further determine whether ODVs of vAc51KO were able to initiate infection in the midgut epithelia, total RNA was extracted from the guts of vAc51KO-infected, vAcWT-infected, or uninfected larvae at 18 h after oral infection, and the transcripts of the *gp64*, *pe38*, *gfp*, and *actin* genes were detected by RT-PCR. As shown in Fig. 10C, transcripts of the *gp64*, *pe38,* and *gfp* genes were detectable in the guts of vAcWT-infected larvae but not in the guts of vAc51KO-infected or uninfected larvae. The transcripts of the *actin* gene were detected in all samples and as a control. Taken together, these results demonstrate that *ac51* is essential for the virulence of AcMNPV *in vivo*.

DISCUSSION

AcMNPV *ac51* is conserved in all alphabaculoviruses except Operophtera brumata nucleopolyhedrovirus, but the function of the gene in the viral life cycle is unknown. In this study, we investigated the role of *ac51* in AcMNPV-infected Sf9 cells. Our results demonstrated that *ac51* is not an essential gene for viral replication, but deletion of the gene substantially reduced BV production. More importantly, we found that Ac51 is a nucleocapsid protein that plays an important role in efficient egress of nucleocapsids from the nucleus to the Cyt.

***ac51* is a nonessential gene *in vitro*.** Analysis of vAc51KO-transfected Sf9 cells indicated that *ac51* is not an essential gene for AcMNPV replication; however, BV production was reduced by approximately 99.9% upon deletion of *ac51* (Fig. 2). *Bm40* is the orthologous gene of *ac51* in BmNPV. However, *bm40* was found to be an essential

gene because its deletion abrogated BV production in BmN cells in studies by both Ono et al. and Shen et al. (32, 34). Regarding the Ono et al. study, this discrepancy may be due to the difference in the deletion region between *ac51* and *bm40* in the corresponding virus genomes, because a *CmR* gene was inserted just 1 nt upstream of the initiation codon of the *lef8* gene in the *bm40* deletion mutant, and the effect of the deletion was not confirmed by a repair virus (32). Since *lef8* is an essential gene (51), insertion of *CmR* may affect the transcription initiation of BmNPV *lef8* and lead to a lethal phenotype of *bm40* deletion. In our study, insertion of a *CmR* cassette to disrupt *ac51* expression did not affect the expression of neighboring genes and other AcMNPV genes, because the effect of the deletion was confirmed by a repair virus (Fig. 2).

In the Shen et al. study, the phenotype of the *bm40* deletion mutant was also confirmed using a repair virus, indicating that deletion did not affect the expression of neighboring genes. Some additional differences and some similarities were identified between the results of our study on Ac51 and those of the recently published study by Shen et al. on Bm40. The similarities include results showing that both Bm40 and Ac51 are localized predominantly in the nuclei of infected cells, and deletion of either gene did not affect viral DNA replication or nucleocapsid assembly. The differences between the results of the two studies include the lack of infectious BVs detected by the $TCID_{50}$ endpoint dilution assay upon *bm40* deletion. Additionally, ODVs were not observed in BmN cells transfected with the *bm40*-null bacmid, while *ac51* deletion substantially decreased but did not completely prevent BV production. In addition, intranuclear microvesicle and mature ODV formation were observed in infected Sf9 cells.

The difference in BV production may result from the different measurement methods. In the Shen et al. study, BV production of the *bm40* deletion mutant was determined by $TCID_{50}$ assay depending on the fluorescence of a VP39-enhanced green fluorescent protein (EGFP) fusion protein expressed under an unindicated promoter, while in our study, BV production of vAc51KO was determined by $TCID_{50}$ assay depending on the fluorescence of EGFP expressed under the AcMNPV *ie1* promoter (Fig. 2) and was confirmed by Western blot analysis (Fig. 8A). Alternatively, although AcMNPV and BmNPV are closely related, these differences may result from the differences between the AcMNPV/Sf9 and BmNPV/BmN cell systems. To date, two other genes have been found to show discrepancies in knockout phenotypes between AcMNPV and BmNPV. *gp41* is essential for AcMNPV replication (52) but is not essential for BmNPV replication (32). Furthermore, deletion of *ac79* reduced BV production in AcMNPV (53), while the *ac79* ortholog *bm65* is essential for BmNPV replication (54). Potentially, cell physiology, the mechanisms by which cells respond to viral infection, or cell-specific factors may influence the functions of orthologous proteins in virus-infected cells.

Ac51 is a component of both BVs and ODVs. In addition to the canonical late gene promoter ATAAG, *ac51* also initiates transcription from another atypical promoter element, CGTTA, in AcMNPV-infected Sf9 cells, but no TATA box element is associated with CGTTA (Fig. 1B). Further analysis showed that *ac51* requires viral DNA replication for expression, indicating that *ac51* is a viral late gene. Most baculovirus late genes encode viral structural proteins. While proteomic analysis of the BV and ODV structural proteins of AcMNPV identified Ac51 from BVs but not from ODVs (27, 28), our study demonstrated that Ac51 is associated with both BVs and ODVs and is a nucleocapsid component of BVs (Fig. 6), which is consistent with the localization of Sl39 (31). Moreover, Bm40 and Ha39 have also been detected in ODVs by mass spectrometry (30, 33). Several possible reasons may explain why Ac51 was not detected in ODVs by proteomic analysis. First, one of the methods used in the Braunagel et al. study involved screening ODV-specific proteins from an expression library of the AcMNPV genome, and both BV- and ODV-associated proteins were excluded; therefore, Ac51 may have been excluded from the analysis. Second, some limitations may be associated with the applied techniques, preventing the identification of all the ODV components. Finally, Ac51 may be a low-abundance protein and may be difficult to detect with the applied

methods. Other examples of baculoviral proteins that have been demonstrated to be ODV components but were not identified by proteomic analysis include Ac141 (20), ME53 (55), and Ac75 (13).

In addition to Ac51, some viral structural proteins are involved in the nuclear egress of AcMNPV nucleocapsids. Some BV-associated proteins have already been found to be required for the nuclear egress of nucleocapsids for the formation of BVs, namely, Ac93 (15), Ac75 (13), Ac76 (17), Ac142 (18), Ac66 (19), and Ac141 (20). These proteins seem to belong to two categories. (i) Ac93 and Ac75 are components of both the nucleocapsids and envelopes of BVs, while Ac76 is an envelope component and Ac142 is a nucleocapsid component. Deletion of each of these genes did not affect nucleocapsid assembly but prevented the nuclear egress of nucleocapsids, thus abrogating BV production. Meanwhile, deletion of the genes also interrupted the formation of ODVs (13, 15, 17, 18). (ii) Deletion of either *ac66* or *ac141* did not affect nucleocapsid assembly but decreased the efficiency of the nuclear egress of nucleocapsids substantially, resulting in decreased BV production (reduced by approximately 5,000-fold and 10,000-fold, respectively). In contrast to the gene knockout phenotype of the first category, neither of the deletions prevented ODV formation (19, 20). The present study indicates that Ac51 is a third identified nucleocapsid protein belonging to the second category; this protein is specifically required for the nuclear egress of nucleocapsids but is not essential for nucleocapsid assembly or ODV formation. Interestingly, according to a recent report on Bm40, which is essential for the nuclear egress of nucleocapsids and ODV formation, this Ac51 ortholog in BmNPV belongs to the first category. Although mass spectrometric analysis showed that Bm40 is a component of ODVs (33), whether Bm40 is a component of BVs remains unknown.

Similar to Ac141 and Ac66, Ac51 is also a component of both BVs and ODVs (Fig. 6) and is a nucleocapsid protein of BVs (20, 27, 28, 56). In addition, Ac51, Ac141, and Ac66 are all localized in both the Cyt and the nuclei of infected Sf9 cells throughout the infection period. Therefore, these three proteins may cooperate via a common pathway for BV maturation. Orthologous genes of *ac51* or *ac141* are found only in alphabaculoviruses. Although *ac141* orthologs have also been found in betabaculoviruses, the sequences of these orthologs share low similarity with the *ac141* sequence, implying that Ac141 has a specific function in alphabaculoviruses. The functions of these two proteins in promoting BV production may be one explanation for the low BV titer of betabaculoviruses in cultured cell lines, suggesting that the acquisition of *ac141* and *ac51* may be important for the evolution of alphabaculoviruses.

Possible mechanisms by which viral structural proteins are involved in the nuclear egress of nucleocapsids. As shown by TEM in our study and other studies (13, 20), baculovirus nucleocapsids seem to pass through the NM to the Cyt by a budding process, but the mechanism by which viral structural proteins are involved in this process remains unknown. Viral proteins, including Ac11, Ac76, Ac78, GP41, Ac93, Ac103, Ac142, and Ac146, which are essential for nucleocapsid egress from the nucleus and ODV formation, have recently been shown to interact with the soluble cellular NSF (N-ethylmaleimide-sensitive factor) and ESCRT-III (endosomal sorting complex required for transport) proteins directly or indirectly (11, 57). NSF functions by triggering the fusion of transport vesicles with their target membranes, and ESCRT-III is essential for membrane remodeling and is part of the scission machinery for sorting ubiquitinated membrane proteins into intraluminal vesicles. These viral proteins have been speculated to form a complex to direct nucleocapsids to the Ac76-rich budding region on the NM and to recruit ESCRT-III proteins to promote the nuclear egress of nucleocapsids, and NSF may help cleave vesicles containing progeny nucleocapsids during nuclear egress (11, 14, 57).

To date, Ac141 and Ac66 are the only two viral structural proteins that have been found to be required for efficient nuclear egress of nucleocapsids (19, 20). Ac141 was the first to be identified and is the most studied. The protein has been shown to interact with two other nucleocapsid proteins (BV/ODV-C42 and FP25K) (20, 58). Intriguingly, further studies have indicated that Ac141, as well as VP39, is associated with β-tubulin

and kinesin-1 (a motor protein of microtubules) of cellular microtubule systems, which are required for anterograde trafficking of AcMNPV nucleocapsids in the Cyt of infected Sf9 cells (10, 21, 59). Ac141, together with VP39, BV/ODV-C42, and FP25K, can be coimmunoprecipitated with kinesin-1. However, a yeast two-hybrid assay showed no direct interaction between kinesin-1 and Ac141 or VP39, suggesting that either other nucleocapsid proteins or adapter proteins are required for mediation of the interaction and to promote nucleocapsid transport along microtubules (10). A recent study on the correlation between Ac141 and Ac66 showed that nucleocapsids in BVs, but not ODVs, are specifically ubiquitinated, and the nucleocapsid protein Ac66 and high-molecular-weight conjugates in BVs are also ubiquitinated. Ac141, which is a potential E3 ubiquitin ligase, has been demonstrated to interact with Ac66 and to colocalize with Ac66 and viral ubiquitin at the nuclear periphery, suggesting that the roles of Ac141 and Ac66 in nucleocapsid ubiquitination determine the fate of nucleocapsids in the formation of BVs or ODVs (56). In conclusion, Ac141 appears to be a multifunctional protein and participates in several processes associated with BV morphogenesis by interacting with microtubules and other BV nucleocapsid proteins, including FP25K, BV/ODV-C42, VP39, and Ac66.

Since *ac51* deletion did not interrupt intranuclear microvesicle and ODV formation, the encoded protein may not be a component of the complex mentioned above. Given that deletion of *ac141*, *ac66*, or *ac51* showed similar viral phenotypes and that Ac141 interacts with Ac66, Ac51 may cooperate with Ac141 and Ac66 to promote efficient nuclear egress of nucleocapsids through a different mechanism. Whether Ac51 is also involved in nucleocapsid ubiquitination requires further investigation.

***ac51* is essential for *in vivo* infectivity.** In the present study, viral gene transcripts were not detected in the midgut of *S. exigua* larvae treated with vAc51KO OBs at 18 h after oral infection (Fig. 10C). Two possibilities may explain this observation. First, the ODVs of vAc51KO may not be able to establish the primary infection in midgut epithelial cells. Alternatively, the nucleocapsids released from ODVs of vAc51KO may enter epithelial cells, but due to the lack of Ac51, the newly synthesized nucleocapsids are mostly restricted within the nuclei, according to our findings. Thus, BV production was too low to spread the infection to other midgut epithelial cells. Moreover, the infected epithelial cells may have been exfoliated by sloughing or molting of the hosts (60). Therefore, the viral transcript levels in the midgut epithelia were too low to be detected by RT-PCR. Regardless of the possibilities, our results demonstrated that ODVs of vAc51KO were unable to establish systemic infection and lost virulence in *S. exigua* (Table 3 and Fig. 10B).

Conserved domains of Ac51 and their potential importance to Ac51 function. Sequence-based computational prediction has shown that Ac51 and most of its orthologs contain an N-terminal DnaJ domain, an RNA recognition motif, and a coiled-coil domain (29, 31, 34), and Ac51 has been known as the DnaJ protein of baculovirus (2). In our study, we found that an *ac51* repair virus constructed by inserting an N-terminally hemagglutinin (HA)-tagged Ac51 into the *polh* locus of bAc51KO could not rescue virus replication completely (data not shown), suggesting that the HA tag may affect the function of Ac51 and that the N terminus of Ac51 is important. In addition, deletion of the DnaJ domain of Bm40 resulted in no infectious BVs (34). These results suggest the importance of the DnaJ domain for Ac51 and Bm40 function. The RNA recognition motifs may not be crucial, as their deletion in Bm40 had no significant effect on BV production (34). Since both Ac141 and Ac51 contain coiled-coil domains (34, 56), which are among the principal oligomerization motifs in proteins (61–63), whether Ac51 interacts with Ac141 via coiled-coil domains and whether this interaction promotes anterograde transport of nucleocapsids would be interesting to investigate.

MATERIALS AND METHODS

Cells, viruses, bacmids, and the anti-Ac51 antibody. *S. frugiperda* IPLB-Sf21-AE clonal isolate 9 (Sf9) cells were cultured at 27°C in TNM-FH medium (Invitrogen) supplemented with 10% fetal bovine serum, penicillin (100 μg/ml), and streptomycin (30 μg/ml). The bacmid bMON14272 (Invitrogen), which is a shuttle vector and contains an AcMNPV genome (64), was used to generate AcMNPV recombinants.

DH10Bac cells, which contained bMON14272, pBAD-gbaA (encoding recombinase) (65), and the helper plasmid pMON7124 (encoding transposase) (64), were used for homologous recombination and transposition. In all the experiments, the cells were allowed to adsorb the viral inocula for 1 hpi or 5 hpt at 27°C, and then the medium was replaced with fresh medium. Time zero was defined as the time when the viral inocula were replaced. Bacmid DNA was isolated using a Qiagen Large-Construct kit (Qiagen). A polyclonal antibody against Ac51 was prepared in rabbits by Abmart (Shanghai, China). Specifically, full-length Ac51 protein was purified from *Escherichia coli* and used to immunize rabbits. The anti-Ac51 antibody was then purified from rabbit serum and verified by Western blot analysis and enzyme-linked immunosorbent assay (ELISA).

RT-PCR and 5′ RACE analyses. Sf9 cells (1.0×10^6) were infected with wild-type AcMNPV at an MOI of 5 $TCID_{50}$/cell and harvested at various time points postinfection. Total cellular RNA was extracted using an RNeasy Mini kit (Qiagen) and digested with RNase-free DNase (Promega) to eliminate DNA contamination. cDNA was synthesized using a iScript cDNA synthesis kit (Bio-Rad) according to the manufacturer's instructions. Subsequently, *ac51*-, *pe38*-, *gp64*-, or *vp39*-specific transcripts were amplified with the primer pairs 515/513, pe385/pe383, gp645/gp643, and vp395/vp393 (the sequences of all the primers used in this study are shown in Table 1), respectively, using the cDNA as a template.

To map the transcription start site of *ac51*, total RNA was isolated from wild-type AcMNPV-infected Sf9 cells at 6 and 24 hpi. The 5′ RACE reaction was performed using a FirstChoice RLM-RACE kit (Ambion) according to the manufacturer's protocol. Two *ac51*-specific primers, namely, 51sp1 and 51sp2, together with the adapter primers provided in the kit, were used to amplify the 5′ ends of *ac51*-specific transcripts. The PCR products were cloned into the pMD18-T vectors (TaKaRa) and sequenced.

Construction of an *ac51* knockout AcMNPV. An *ac51* knockout bacmid was generated as follows. Using the primer pair 51L5/51L3 and the template pUC18-Cm (66), a 1,137-bp fragment was amplified by PCR. The fragment contained a 1,038-bp *CmR* cassette and 49-bp and 50-bp fragments flanking the deletion region at its 5′ and 3′ ends, respectively. Then, the fragment was transformed into electrocompetent DH10Bac cells to replace the N-terminal 125-bp (nt 43514 to 43638 of the AcMNPV genome) of *ac51* with the *CmR* cassette via λ Red homologous recombination, as previously described (67). The resulting *ac51* knockout bacmid was designated bAc51KO.

To facilitate the examination of viral infection, an AcMNPV *polh* gene under its native promoter and an *egfp* gene under the AcMNPV *ie1* promoter were inserted into the *polh* locus of bAc51KO via Tn*7*-mediated transposition by transforming chemically competent DH10B cells containing bAc51KO and pMON7124 with the donor plasmid pFB1-PH-GFP (66), as previously described (66). The generated *ac51* knockout virus was named vAc51KO. A wild-type control virus was generated by inserting the *polh* and *egfp* genes into the *polh* locus of bMON14272 and named vAcWT.

To generate an Ac51 repair virus, the donor plasmid pFB1-Ac51-PH-GFP was first constructed as follows. A 1,404-bp fragment containing the *ac51* native promoter and open reading frame (ORF) was amplified by PCR from bMON14272 using the primers 51P5 and 51rep3. The PCR products were digested with SacI and BamHI and ligated into pUC18-SV40 (68) to generate pUC18-Ac51-SV40. pUC18-Ac51-SV40 was then digested with SacI and XbaI, and the Ac51-SV40 fragment was cloned into pFB1-PH-GFP to generate pFB1-Ac51-PH-GFP. pFB1-Ac51-PH-GFP was transformed into chemically competent DH10B cells containing bAc51KO and pMON7124 to generate an Ac51-repaired virus via Tn*7*-mediated transposition, and the virus was designated vAc51REP. All of the recombinants were verified by PCR and sequencing.

Viral growth curves and plaque assays. Sf9 cells (1.0×10^6) were transfected with 1.0 μg of vAc51KO, vAc51REP, or vAcWT bacmid DNA, or Sf9 cells (5.0×10^5) were infected with vAc51KO, vAc51REP, or vAcWT bacmid DNA at an MOI of 0.2 $TCID_{50}$/cell. At various time points posttransfection, cell supernatants were harvested, and infectious BV production was determined based on a $TCID_{50}$ endpoint dilution assay in Sf9 cells (69). Plaque assays were performed as previously described (69). Specifically, a total of 1.8×10^6 cells in a monolayer were transfected with 0.2 μg of vAc51KO, vAc51REP, or vAcWT bacmid DNA. At 120 hpt, the viral plaques were photographed and measured.

qPCR. To evaluate the effect of the *ac51* deletion on viral DNA replication, qPCR analysis was performed using the AcMNPV *gp41* gene copies to represent the viral genome copies, as previously described (45). Sf9 cells (1.0×10^6) were transfected with 0.5 μg of vAc51KO or vAc51REP bacmid DNA and harvested at various time points posttransfection. Total cellular DNA was isolated using a Universal Genomic DNA extraction kit version 5.0 (TaKaRa). The DNA (1 μg) was then digested with DpnI (TaKaRa) overnight to remove any residual bacmid DNA introduced during transfection. qPCR was performed using TranStart SYBR Green qPCR SuperMix (TranGen Biotech) and a StepOnePlus real-time PCR system (Applied Biosystem). The *gp41* primer set (gp41F/gp41R) was used to amplify part of the *gp41* sequence under the following conditions: 95°C for 2 min, followed by 40 cycles of 95°C for 15 s and 60°C for 30 s. Purified AcMNPV bacmid DNA from the bacteria was serially diluted from 53 μg/ml to 5.3×10^{-7} μg/ml to generate a standard curve.

RT-qPCR. RT-qPCR was performed to evaluate the effect of *ac51* deletion on viral gene transcription. Sf9 cells (1.0×10^6) were transfected with 0.5 μg of vAc51KO or vAcWT bacmid DNA and harvested at 24 hpt. Total cellular RNA was isolated using a Universal Genomic RNA extraction kit (TaKaRa). cDNA was synthesized as described above. Six viral genes were selected to represent the immediate-early, delayed-early, or late genes. qPCR was conducted as described above with cDNA as the template to determine gene transcript levels using the corresponding primer pairs. Host 18S rRNA was selected, and the transcript levels of the RNA were determined as the endogenous reference values (70).

Western blot analysis. To analyze the temporal expression of Ac51, Sf9 cells (1.0×10^6) were infected with vAcWT at an MOI of 10 $TCID_{50}$/cell, scraped at various time points, and centrifuged at

6,000 rpm for 5 min at 4°C. The cell pellets were then resuspended in 40 μl of phosphate-buffered saline (PBS), mixed with 10 μl of 5× protein loading buffer, and incubated at 100°C for 10 min. After centrifugation at 12,000 rpm for 5 min, 30-μl aliquots of the supernatants were resolved by SDS-12% PAGE and transferred onto a polyvinylidene difluoride (PVDF) membrane (Millipore). Western blot analysis was performed using an antibody raised against Ac51 as the primary antibody (1:1,000) and a horseradish peroxidase (HRP)-conjugated donkey anti-rabbit antibody (1:5,000; Promega) as the secondary antibody. The signals were detected using an electrochemical luminescence system (Amersham Biosciences) according to the manufacturer's instructions.

To analyze whether *ac51* is an early or late viral gene, Sf9 cells (1.0×10^6) were infected with vAcWT at an MOI of 5 $TCID_{50}$/cell, and the DNA synthesis inhibitor aphidicolin (dissolved in dimethyl sulfoxide [DMSO]) at 5 μg/ml (71) or DMSO only was added to the cells during infection and maintained thereafter. The cells were scraped at 24 hpi and prepared as described above. Then, 20-μl aliquots of the supernatants were resolved by SDS-10% PAGE. Western blot analysis was performed using a mouse monoclonal anti-GP64 antibody (1:2,000; eBioscience), a rabbit polyclonal antibody against AcMNPV VP39 (1:1,000 [72]), the anti-Ac51 antibody (1:1,000), or a mouse monoclonal anti-actin antibody (1:2,000; Proteintech Group) as the primary antibody. An HRP-conjugated goat anti-mouse antibody (1:5,000; Amersham Biosciences) or an HRP-conjugated donkey anti-rabbit antibody served as the secondary antibody.

To analyze the syntheses of the viral proteins GP64, VP39, and P6.9, Sf9 cells (1.0×10^6) were transfected with 0.5 μg of vAc51KO or vAcWT bacmid DNA. At various times posttransfection, the cells were scraped and centrifuged at 6,000 rpm for 5 min at 4°C. After being lysed in radioimmunoprecipitation assay (RIPA) lysis buffer (Thermo Scientific), the cells were centrifuged at 12,000 rpm for 10 min at 4°C. The supernatants were collected, and the protein concentrations were determined using a bicinchoninic acid (BCA) protein assay kit (Thermo Scientific). Then, 50 μg of the total protein from each sample was mixed with 5× protein loading buffer and then treated and subjected to Western blot analysis as described above. The primary antibodies used were the anti-GP64 antibody (1:4,000), the anti-VP39 antibody (1:2,000), a rabbit polyclonal antibody against AcMNPV P6.9 (1:4,000 [73]), and a mouse monoclonal anti-actin antibody (1:2,000; Abmart). The secondary antibodies used are described above.

To analyze the localization of Ac51 in virions, BVs and ODVs were purified, and the BVs were fractionated into nucleocapsid and envelope fractions as previously described (15). Protein samples were then subjected to Western blot analysis. The anti-Ac51 antibody (1:1,000), anti-VP39 antibody (1:1,000), or anti-GP64 antibody (1:2,000) was used as the primary antibody, and the secondary antibodies used are described above.

For analysis of total BV production in the culture supernatants of vAc51KO- or vAcWT-transfected cells at 24 hpt, BVs were first purified from equal volumes of the supernatants and then subjected to Western blot analysis. The anti-GP64 antibody (1:2,000) or anti-VP39 antibody (1:1,000) was used as the primary antibody, and the secondary antibodies used are described above.

Immunofluorescence. Immunofluorescence was performed as previously described (15). Sf9 cells (1.0×10^6) were infected with vAcWT at an MOI of 5 $TCID_{50}$/cell. At various time points, the cells were probed with the anti-Ac51 antibody (1:200), incubated with an Alexa Fluor 555-conjugated donkey anti-rabbit secondary antibody (1:500; Invitrogen), and subsequently stained with Hoechst 33342 (1:1,000; Sigma). Subcellular localization of Ac51 was examined with a Zeiss7 Duo NLO confocal microscope.

IEM. Sf9 cells were infected with vAcWT at an MOI of 5 $TCID_{50}$/cell, collected at 72 hpi, and pelleted at 1,000 × *g* for 5 min. The cells were then prepared for IEM with LR White resin (Ted Pella, Inc.) as previously described (14). The anti-Ac51 antibody was used as the primary antibody (1:50), and a goat anti-rabbit antibody conjugated to 10-nm gold particles (1:50; Sigma) was used as the secondary antibody. The samples were visualized and photographed with a JEOL JEM-1400 transmission electron microscope.

TEM. To analyze the effect of *ac51* deletion on viral morphogenesis, Sf9 cells (1.0×10^6) were transfected with vAc51KO or vAcWT bacmid DNA. At various time points posttransfection, cells were collected and prepared for TEM as previously described (74). All the sections were examined and photographed with a JEOL JEM-1400 or JEM-100CX-II transmission electron microscope. To analyze nucleocapsid egress, 10 intact vAc51KO-transfected cells and 10 intact vAcWT-transfected cells were observed and photographed at each time point (i.e., 36, 48, and 72 hpt). The nucleocapsids in the nucleus or during egress in each cell were counted using Adobe Photoshop CS6.

***In vivo* infectivity assay.** The infectivity of vAc51KO ODVs *in vivo* was determined by orally infecting newly molted 3rd-instar *S. exigua* larvae with OBs as previously described (75, 76). Specifically, OBs of vAc51KO or vAcWT were purified from Sf9 cells transfected with bacmid DNA of vAc51KO or vAcWT, respectively, and quantified. The *S. exigua* larvae were infected by allowing them to consume food treated with H_2O or OBs (4×10^4 OBs/larva) for 12 h. Infected larvae were reared individually in 12-well plates and monitored daily until all the larvae died or pupated. A cohort of 16 larvae was used for each treatment, and the treatment was repeated in triplicate. Larvae that were dead and exhibited an entirely black body for unknown reasons within 3 days were excluded.

One separate experiment was conducted to examine whether systemic infection was established in treated larvae. Each larva was orally fed 4×10^4 OBs or H_2O. The hemolymph of each larva was collected 5 days after oral infection, dropped on a slide, and examined with a fluorescence microscope (Nikon Eclipse TE2000-U). Another separate experiment was conducted to examine whether the primary infection was established. The guts of seven larvae treated with H_2O or OBs (4×10^4 OBs/larva) were dissected 18 h after oral infection, and total RNA was extracted using the TRIzol-phenol chloroform

method. RT-PCR was then performed to detect the transcripts of the *pe38*, *gp64*, *gfp*, and *actin* genes using the primer pairs pe385/pe383, gp645/gp643, gfpF/gfpR, and actinF/actinR, as indicated in Table 1.

ACKNOWLEDGMENTS

This research was supported by the National Key R&D Program of China (2017YFD0200400) and the Guangzhou Science and Technology Project (201707020003).

REFERENCES

1. Miranda-Saksena M, Denes CE, Diefenbach RJ, Cunningham AL. 2018. Infection and transport of herpes simplex virus type 1 in neurons: role of the cytoskeleton. Viruses 10:E92. https://doi.org/10.3390/v10020092.
2. Rohrmann GF. 2013. Baculovirus molecular biology, 3rd ed. National Center for Biotechnology Information, Bethesda, MD.
3. Schudt G, Dolnik O, Kolesnikova L, Biedenkopf N, Herwig A, Becker S. 2015. Transport of ebolavirus nucleocapsids is dependent on actin polymerization: live-cell imaging analysis of ebolavirus-infected cells. J Infect Dis 212(Suppl 2):S160–S166. https://doi.org/10.1093/infdis/jiv083.
4. Herniou EA, Arif BM, Becnel JJ, Blissard GW, Bonning B, Harrison JR, Theilmann DA, Vlka JM. 2012. Family Baculoviridae, p 163–173. *In* King AMQ, Adams MJ, Carstens EB, Lefkowitz EJ (ed), Virus taxonomy. Classification and nomenclature of viruses. 9th report of the International Committee on Taxonomy of Viruses. Elsevier Academic Press, San Diego, CA.
5. Herniou EA, Olszewski JA, Cory JS, O'Reilly DR. 2003. The genome sequence and evolution of baculoviruses. Annu Rev Entomol 48:211–234. https://doi.org/10.1146/annurev.ento.48.091801.112756.
6. Lu A, Miller LK. 1997. Regulation of baculovirus late and very late gene expression, p 193–216. *In* Miller LK (ed), The baculoviruses. Springer, Boston, MA.
7. Friesen PD. 1997. Regulation of baculovirus early gene expression, p 141–170. *In* Miller LK (ed), The baculoviruses. Springer, Boston, MA.
8. Williams GV, Faulkner P. 1997. Cytological changes and viral morphogenesis duriing baculovirus infection, p 61–107. *In* Miller LK (ed), The baculoviruses. Springer, Boston, MA.
9. Marek M, Merten OW, Galibert L, Vlak JM, van Oers MM. 2011. Baculovirus VP80 protein and the F-actin cytoskeleton interact and connect the viral replication factory with the nuclear periphery. J Virol 85:5350–5362. https://doi.org/10.1128/JVI.00035-11.
10. Biswas S, Blissard GW, Theilmann DA. 2016. Trichoplusia ni kinesin-1 associates with AcMNPV nucleocapsid proteins and is required for the production of budded virus. J Virol 90:3480–3495. https://doi.org/10.1128/JVI.02912-15.
11. Yue Q, Yu Q, Yang Q, Xu Y, Guo Y, Blissard GW, Li Z. 2017. Distinct roles of cellular ESCRT-I and ESCRT-III proteins in efficient entry and egress of budded virions of Autographa californica multiple nucleopolyhedrovirus. J Virol 92:e01636-17. https://doi.org/10.1128/JVI.01636-17.
12. Marek M, van Oers MM, Devaraj FF, Vlak JM, Merten OW. 2011. Engineering of baculovirus vectors for the manufacture of virion-free biopharmaceuticals. Biotechnol Bioeng 108:1056–1067. https://doi.org/10.1002/bit.23028.
13. Shi A, Hu Z, Zuo Y, Wang Y, Wu W, Yuan M, Yang K. 2018. Autographa californica multiple nucleopolyhedrovirus ac75 is required for the nuclear egress of nucleocapsids and intranuclear microvesicle formation. J Virol 92:e01509-17. https://doi.org/10.1128/JVI.01509-17.
14. Wei D, Wang Y, Zhang X, Hu Z, Yuan M, Yang K. 2014. Autographa californica nucleopolyhedrovirus Ac76: a dimeric type II integral membrane protein that contains an inner nuclear membrane-sorting motif. J Virol 88:1090–1103. https://doi.org/10.1128/JVI.02392-13.
15. Yuan M, Huang Z, Wei D, Hu Z, Yang K, Pang Y. 2011. Identification of Autographa californica nucleopolyhedrovirus ac93 as a core gene and its requirement for intranuclear microvesicle formation and nuclear egress of nucleocapsids. J Virol 85:11664–11674. https://doi.org/10.1128/JVI.05275-11.
16. Tao XY, Choi JY, Kim WJ, An SB, Liu Q, Kim SE, Lee SH, Kim JH, Woo SD, Jin BR, Je YH. 2015. Autographa californica multiple nucleopolyhedrovirus ORF11 is essential for budded-virus production and occlusion-derived-virus envelopment. J Virol 89:373–383. https://doi.org/10.1128/JVI.01742-14.
17. Hu Z, Yuan M, Wu W, Liu C, Yang K, Pang Y. 2010. Autographa californica multiple nucleopolyhedrovirus ac76 is involved in intranuclear microvesicle formation. J Virol 84:7437–7447. https://doi.org/10.1128/JVI.02103-09.
18. McCarthy CB, Dai X, Donly C, Theilmann DA. 2008. Autographa californica multiple nucleopolyhedrovirus ac142, a core gene that is essential for BV production and ODV envelopment. Virology 372:325–339. https://doi.org/10.1016/j.virol.2007.10.019.
19. Ke J, Wang J, Deng R, Wang X. 2008. Autographa californica multiple nucleopolyhedrovirus ac66 is required for the efficient egress of nucleocapsids from the nucleus, general synthesis of preoccluded virions and occlusion body formation. Virology 374:421–431. https://doi.org/10.1016/j.virol.2007.12.033.
20. Fang M, Dai X, Theilmann DA. 2007. Autographa californica multiple nucleopolyhedrovirus EXON0 (ORF141) is required for efficient egress of nucleocapsids from the nucleus. J Virol 81:9859–9869. https://doi.org/10.1128/JVI.00588-07.
21. Danquah JO, Botchway S, Jeshtadi A, King LA. 2012. Direct interaction of baculovirus capsid proteins VP39 and EXON0 with kinesin-1 in insect cells determined by fluorescence resonance energy transfer-fluorescence lifetime imaging microscopy. J Virol 86:844–853. https://doi.org/10.1128/JVI.06109-11.
22. Oomens AG, Blissard GW. 1999. Requirement for GP64 to drive efficient budding of Autographa californica multicapsid nucleopolyhedrovirus. Virology 254:297–314. https://doi.org/10.1006/viro.1998.9523.
23. Monsma SA, Oomens AG, Blissard GW. 1996. The GP64 envelope fusion protein is an essential baculovirus protein required for cell-to-cell transmission of infection. J Virol 70:4607–4616.
24. Jehle JA, Blissard GW, Bonning BC, Cory JS, Herniou EA, Rohrmann GF, Theilmann DA, Thiem SM, Vlak JM. 2006. On the classification and nomenclature of baculoviruses: a proposal for revision. Arch Virol 151:1257–1266. https://doi.org/10.1007/s00705-006-0763-6.
25. Federici BA. 1997. Baculovirus pathogenesis, p 33–59. *In* Miller LK (ed), The baculoviruses. Springer, Boston, MA.
26. Winstanley D, Crook NE. 1993. Replication of Cydia pomonella granulosis virus in cell cultures. J Gen Virol 74:1599–1609. https://doi.org/10.1099/0022-1317-74-8-1599.
27. Wang R, Deng F, Hou D, Zhao Y, Guo L, Wang H, Hu Z. 2010. Proteomics of the Autographa californica nucleopolyhedrovirus budded virions. J Virol 84:7233–7242. https://doi.org/10.1128/JVI.00040-10.
28. Braunagel SC, Russell WK, Rosas-Acosta G, Russell DH, Summers MD. 2003. Determination of the protein composition of the occlusion-derived virus of Autographa californica nucleopolyhedrovirus. Proc Natl Acad Sci U S A 100:9797–9802. https://doi.org/10.1073/pnas.1733972100.
29. Xu HJ, Liu YH, Yang ZN, Zhang CX. 2006. Characterization of ORF39 from Helicoverpa armigera single-nucleocapsid nucleopolyhedrovirus, the gene containing RNA recognition motif. J Biochem Mol Biol 39:263–269.
30. Hou D, Zhang L, Deng F, Fang W, Wang R, Liu X, Guo L, Rayner S, Chen X, Wang H, Hu Z. 2013. Comparative proteomics reveal fundamental structural and functional differences between the two progeny phenotypes of a baculovirus. J Virol 87:829–839. https://doi.org/10.1128/JVI.02329-12.
31. Wang L, Yu J, Yin C, Li Z, Hu X, Pang Y. 2002. Characterization of a J domain gene of Spodoptera litura multicapsid nucleopolyhedrovirus. Virus Genes 25:291–297. https://doi.org/10.1023/A:1020980109450.
32. Ono C, Kamagata T, Taka H, Sahara K, Asano S, Bando H. 2012. Phenotypic grouping of 141 BmNPVs lacking viral gene sequences. Virus Res 165:197–206. https://doi.org/10.1016/j.virusres.2012.02.016.
33. Liu X, Chen K, Cai K, Yao Q. 2008. Determination of protein composition and host-derived proteins of Bombyx mori nucleopolyhedrovirus by 2-dimensional electrophoresis and mass spectrometry. Intervirology 51:369–376. https://doi.org/10.1159/000193462.

34. Shen Y, Feng M, Wu X. 2018. Bombyx mori nucleopolyhedrovirus ORF40 is essential for budded virus production and occlusion-derived virus envelopment. J Gen Virol 99:837–850. https://doi.org/10.1099/jgv.0.001066.
35. Maeda S, Kamita SG, Kondo A. 1993. Host range expansion of Autographa californica nuclear polyhedrosis virus (NPV) following recombination of a 0.6-kilobase-pair DNA fragment originating from Bombyx mori NPV. J Virol 67:6234–6238.
36. Nagamine T, Sako Y. 2016. A role for the anti-viral host defense mechanism in the phylogenetic divergence in baculovirus evolution. PLoS One 11:e0156394. https://doi.org/10.1371/journal.pone.0156394.
37. Herniou EA, Olszewski JA, O'Reilly DR, Cory JS. 2004. Ancient coevolution of baculoviruses and their insect hosts. J Virol 78:3244–3251. https://doi.org/10.1128/JVI.78.7.3244-3251.2004.
38. Berretta MF, Deshpande M, Crouch EA, Passarelli AL. 2006. Functional characterization of Bombyx mori nucleopolyhedrovirus late gene transcription and genome replication factors in the non-permissive insect cell line SF-21. Virology 348:175–189. https://doi.org/10.1016/j.virol.2005.12.017.
39. Hamajima R, Kobayashi M, Ikeda M. 2017. P143 proteins from heterologous nucleopolyhedroviruses induce apoptosis in BM-N cells derived from the silkworm Bombyx mori. Virus Res 233:70–76. https://doi.org/10.1016/j.virusres.2017.03.012.
40. Hamajima R, Kobayashi M, Ikeda M. 2015. Identification of amino acid residues of AcMNPV P143 protein involved in rRNA degradation and restricted viral replication in BM-N cells from the silkworm Bombyx mori. Virology 485:244–251. https://doi.org/10.1016/j.virol.2015.08.008.
41. Hamajima R, Ito Y, Ichikawa H, Mitsutake H, Kobayashi J, Kobayashi M, Ikeda M. 2013. Degradation of rRNA in BM-N cells from the silkworm Bombyx mori during abortive infection with heterologous nucleopolyhedroviruses. J Gen Virol 94:2102–2111. https://doi.org/10.1099/vir.0.053645-0.
42. Jiang SS, Chang IS, Huang LW, Chen PC, Wen CC, Liu SC, Chien LC, Lin CY, Hsiung CA, Juang JL. 2006. Temporal transcription program of recombinant Autographa californica multiple nucleopolyhedrosis virus. J Virol 80:8989–8999. https://doi.org/10.1128/JVI.01158-06.
43. Chen YR, Zhong S, Fei Z, Hashimoto Y, Xiang JZ, Zhang S, Blissard GW. 2013. The transcriptome of the baculovirus Autographa californica multiple nucleopolyhedrovirus in Trichoplusia ni cells. J Virol 87:6391–6405. https://doi.org/10.1128/JVI.00194-13.
44. Ayres MD, Howard SC, Kuzio J, Lopez-Ferber M, Possee RD. 1994. The complete DNA sequence of Autographa californica nuclear polyhedrosis virus. Virology 202:586–605. https://doi.org/10.1006/viro.1994.1380.
45. Vanarsdall AL, Okano K, Rohrmann GF. 2005. Characterization of the replication of a baculovirus mutant lacking the DNA polymerase gene. Virology 331:175–180. https://doi.org/10.1016/j.virol.2004.10.024.
46. Pearson MN, Russell RL, Rohrmann GF, Beaudreau GS. 1988. p39, a major baculovirus structural protein: immunocytochemical characterization and genetic location. Virology 167:407–413. https://doi.org/10.1016/0042-6822(88)90102-X.
47. Wang M, Tuladhar E, Shen S, Wang H, van Oers MM, Vlak JM, Westenberg M. 2010. Specificity of baculovirus P6.9 basic DNA-binding proteins and critical role of the C terminus in virion formation. J Virol 84:8821–8828. https://doi.org/10.1128/JVI.00072-10.
48. DuRaine G, Wisner TW, Howard P, Williams M, Johnson DC. 2017. Herpes simplex virus gE/gI and US9 promote both envelopment and sorting of virus particles in the cytoplasm of neurons, two processes that precede anterograde transport in axons. J Virol 91:e00050-17. https://doi.org/10.1128/JVI.00050-17.
49. Wilkie AR, Lawler JL, Coen DM. 2016. A role for nuclear F-actin induction in human cytomegalovirus nuclear egress. mBio 7:e01254-16. https://doi.org/10.1128/mBio.01254-16.
50. Oda S, Arii J, Koyanagi N, Kato A, Kawaguchi Y. 2016. The interaction between herpes simplex virus 1 tegument proteins UL51 and UL14 and its role in virion morphogenesis. J Virol 90:8754–8767. https://doi.org/10.1128/JVI.01258-16.
51. Shikata M, Sano Y, Hashimoto Y, Matsumoto T. 1998. Isolation and characterization of a temperature-sensitive mutant of Bombyx mori nucleopolyhedrovirus for a putative RNA polymerase gene. J Gen Virol 79:2071–2078. https://doi.org/10.1099/0022-1317-79-8-2071.
52. Li Y, Shen S, Hu L, Deng F, Vlak JM, Hu Z, Wang H, Wang M. 2018. The functional oligomeric state of tegument protein GP41 is essential for baculovirus BV and ODV assembly. J Virol 92:e02083-17. https://doi.org/10.1128/JVI.02083-17.
53. Wu W, Passarelli AL. 2012. The Autographa californica M nucleopolyhedrovirus ac79 gene encodes an early gene product with structural similarities to UvrC and intron-encoded endonucleases that is required for efficient budded virus production. J Virol 86:5614–5625. https://doi.org/10.1128/JVI.06252-11.
54. Tang Q, Li G, Yao Q, Chen L, Feng F, Yuan Y, Chen K. 2013. Bm65 is essential for the propagation of Bombyx mori nucleopolyhedrovirus. Curr Microbiol 66:22–29. https://doi.org/10.1007/s00284-012-0236-y.
55. de Jong J, Arif BM, Theilmann DA, Krell PJ. 2009. Autographa californica multiple nucleopolyhedrovirus me53 (ac140) is a nonessential gene required for efficient budded-virus production. J Virol 83:7440–7448. https://doi.org/10.1128/JVI.02390-08.
56. Biswas S, Willis LG, Fang M, Nie Y, Theilmann DA. 2018. Autographa californica nucleopolyhedrovirus AC141 (Exon0), a potential E3 ubiquitin ligase, interacts with viral ubiquitin and AC66 to facilitate nucleocapsid egress. J Virol 92:e01713-17. https://doi.org/10.1128/JVI.01713-17.
57. Guo Y, Yue Q, Gao J, Wang Z, Chen YR, Blissard GW, Liu TX, Li Z. 2017. Roles of cellular NSF protein in entry and nuclear egress of budded virions of Autographa californica multiple nucleopolyhedrovirus. J Virol 91:e01111-17. https://doi.org/10.1128/JVI.01111-17.
58. Fang M, Nie Y, Dai X, Theilmann DA. 2008. Identification of AcMNPV EXON0 (ac141) domains required for efficient production of budded virus, dimerization and association with BV/ODV-C42 and FP25. Virology 375:265–276. https://doi.org/10.1016/j.virol.2008.01.036.
59. Fang M, Nie Y, Theilmann DA. 2009. AcMNPV EXON0 (AC141) which is required for the efficient egress of budded virus nucleocapsids interacts with beta-tubulin. Virology 385:496–504. https://doi.org/10.1016/j.virol.2008.12.023.
60. Keddie BA, Aponte GW, Volkman LE. 1989. The pathway of infection of Autographa californica nuclear polyhedrosis virus in an insect host. Science 243:1728–1730. https://doi.org/10.1126/science.2648574.
61. Burhard P, Stetefeld J, Strelkov SV. 2001. Coiled coils: a highly versatile protein folding motif. Trends Cell Biol 11:82–88. https://doi.org/10.1016/S0962-8924(00)01898-5.
62. Parry DA, Fraser RD, Squire JM. 2008. Fifty years of coiled-coils and alpha-helical bundles: a close relationship between sequence and structure. J Struct Biol 163:258–269. https://doi.org/10.1016/j.jsb.2008.01.016.
63. Truebestein L, Leonard TA. 2016. Coiled-coils: The long and short of it. Bioessays 38:903–916. https://doi.org/10.1002/bies.201600062.
64. Luckow VA, Lee SC, Barry GF, Olins PO. 1993. Efficient generation of infectious recombinant baculoviruses by site-specific transposon-mediated insertion of foreign genes into a baculovirus genome propagated in Escherichia coli. J Virol 67:4566–4579.
65. Muyrers JP, Zhang Y, Testa G, Stewart AF. 1999. Rapid modification of bacterial artificial chromosomes by ET-recombination. Nucleic Acids Res 27:1555–1557. https://doi.org/10.1093/nar/27.6.1555.
66. Wu W, Lin T, Pan L, Yu M, Li Z, Pang Y, Yang K. 2006. Autographa californica multiple nucleopolyhedrovirus nucleocapsid assembly is interrupted upon deletion of the 38K gene. J Virol 80:11475–11485. https://doi.org/10.1128/JVI.01155-06.
67. Wu W, Passarelli AL. 2010. Autographa californica multiple nucleopolyhedrovirus Ac92 (ORF92, P33) is required for budded virus production and multiply enveloped occlusion-derived virus formation. J Virol 84:12351–12361. https://doi.org/10.1128/JVI.01598-10.
68. Cai Y, Long Z, Qiu J, Yuan M, Li G, Yang K. 2012. An ac34 deletion mutant of Autographa californica nucleopolyhedrovirus exhibits delayed late gene expression and a lack of virulence in vivo. J Virol 86:10432–10443. https://doi.org/10.1128/JVI.00779-12.
69. O'Reilly DR, Miller LK, Luckow VA. 1994. Baculovirus expression vectors: a laboratory manual. Oxford University Press, New York, NY.
70. Peng Y, Li K, Pei RJ, Wu CC, Liang CY, Wang Y, Chen XW. 2012. The protamine-like DNA-binding protein P6.9 epigenetically up-regulates Autographa californica multiple nucleopolyhedrovirus gene transcription in the late infection phase. Virol Sin 27:57–68. https://doi.org/10.1007/s12250-012-3229-x.
71. Detvisitsakun C, Berretta MF, Lehiy C, Passarelli AL. 2005. Stimulation of cell motility by a viral fibroblast growth factor homolog: proposal for a role in viral pathogenesis. Virology 336:308–317. https://doi.org/10.1016/j.virol.2005.03.013.
72. Li L, Li Z, Chen W, Pang Y. 2007. Cloning, expression of Autographa californica nucleopolyhedrovirus vp39 gene in Escherichia coli and preparation of its antibody. Bio/Technology 17:5–7.
73. Liu X, Zhao H, Fang Z, Yuan M, Yang K, Pang Y. 2012. Distribution and phosphorylation of the basic protein P6.9 of Autographa californica

nucleopolyhedrovirus. J Virol 86:12217–12227. https://doi.org/10.1128/JVI.00438-12.
74. Yuan M, Wu W, Liu C, Wang Y, Hu Z, Yang K, Pang Y. 2008. A highly conserved baculovirus gene p48 (ac103) is essential for BV production and ODV envelopment. Virology 379:87–96. https://doi.org/10.1016/j.virol.2008.06.015.
75. Fang M, Nie Y, Harris S, Erlandson MA, Theilmann DA. 2009. Autographa californica multiple nucleopolyhedrovirus core gene ac96 encodes a per os infectivity factor (PIF-4). J Virol 83:12569–12578. https://doi.org/10.1128/JVI.01141-09.
76. Li Q, Li L, Moore K, Donly C, Theilmann DA, Erlandson M. 2003. Characterization of Mamestra configurata nucleopolyhedrovirus enhancin and its functional analysis via expression in an Autographa californica M nucleopolyhedrovirus recombinant. J Gen Virol 84:123–132. https://doi.org/10.1099/vir.0.18679-0.